Market Response to A VIX Impulse*

Nikolaus Hautsch Albert J. Menkveld Stefan Voigt

March 6, 2022

We analyze thirty billion NASDAQ order book messages for four exchange-traded funds to delineate how the market responds to a VIX impulse. We find that investors actively sell equities and buy government bonds on largely unchanged liquidity. Deeper analysis shows that this result is entirely driven by investors becoming more averse to risk. In other words, the pattern we find for VIX impulses is entirely driven by changes in the variance risk premium. For VIX impulses driven by changes in cash-flow risk, we find active *buying* of equities on worse liquidity. We rationalize these patterns by essentially adding risk shocks to Grossman and Stiglitz (1980).

JEL Codes: G11, G12, G20
Keywords: Liquidity, intraday dynamics, big data, exchange-traded funds.

*Nikolaus Hautsch, University of Vienna – Department of Statistics and Operations Research, Research Platform Data Science @ Uni Vienna, Vienna Graduate School of Finance (VGSF) and Center for Financial Studies (CFS), nikolaus.hautsch@univie.ac.at. Albert J. Menkveld, Vrije Universiteit Amsterdam, albertjmenkveld@gmail.com. Stefan Voigt, University of Copenhagen and Danish Finance Institute, stefan.voigt@econ.ku.dk.

1 Introduction

Investors fly to safety at times of elevated risk.[1] They are on high-powered incentives to do so quickly if their liquidity demand exercises a negative externality as a result of a liquidity spiral (Pedersen, 2009; Brunnermeier, 2009). This channel could make markets fragile and, in the extreme, cause financial instability.[2]

To study if and how flight to safety and market fragility are related requires studying market dynamics at high frequencies. We analyze an exhaustive 2007-2021 sample of *all* NASDAQ trading messages for four exchange-traded funds (ETFs). We analyze how VIX shocks affect trading in equity and bond ETFs at a five-minute frequency.

To characterize market dynamics, we estimate generalized impulse response functions. The impulse is a surprise shock in VIX and the response variables include initiator net volume, midquote return, trading volume, bid-ask spread, order book depth, and the Amihud (2002) illiquidity ratio (ILLIQ). We compute these variables for the following ETFs: SPY for the S&P 500 equity index, HYG for junk bonds, LQD for investment-grade corporate bonds, and TLT for government bonds. For ease of exposition, we talk about asset classes instead of referring to ETF codes in the remainder of the manuscript.

Our most salient and most robust finding is that VIX impulses lead to active selling of equities and active buying of government bonds, both contemporaneously and in the hour that follows the shock. Prices drop for equities and increase for government bonds, although only contemporaneously. These price responses revert partially in the subsequent hour, in spite of continued selling of equities and buying of bonds. Market liquidity also responds to VIX impulses, but magnitudes are negligible on all dimensions: bid-ask spread, depth, and ILLIQ.

To study the channel that drives the flight to safety dynamics, we decompose VIX changes into two canonical components:

1. changes in risk aversion, often referred to as variance risk premium (*VRP*), or
2. changes in cash-flow risk, referred to as expected realized volatility (*ERV*).

Although both components could, in principle, cause a flight to safety, we conjecture that *VRP* changes are the most likely triggers. This is in line with a strand of literature that finds time-

[1]See, e.g., Longstaff (2004), Beber et al. (2009), Adrian et al. (2019), Baele et al. (2019).

[2]Central banks worry about market liquidity as part of their focus on liquidity risk management after the global financial crisis (BIS and IOSCO, 2012). The SEC worries about the ramifications of liquidity spirals as evidenced by their 2016 rule that requires each registered open-end management investment company, including open-end exchange-traded funds (ETFs), to establish a liquidity risk management program (SEC, 2016). European regulators share the worry but stopped short of imposing regulation (ESMA, 2019).

varying risk aversion being positively predictive of required returns (Campbell and Cochrane, 1999; Bekaert and Hoerova, 2014; Bollerslev et al., 2015).

To decompose five-minute VIX changes, we develop a high-frequency version of the methodology proposed by Bekaert and Hoerova (2014). We then study how both components relate to all trading variables, both contemporaneously, and subsequently the shock. The findings can be summarized as follows. First off, we find that the two components of VIX changes are close to orthogonal at a five-minute frequency. This is a reassuring result because it allows us to identify potentially different market responses. This turns out to be the case as the responses to the two types of VIX shocks differ markedly. Shocking *VRP* leads to a market response that mirrors the response to VIX shocks. Shocking *ERV*, on the other hand, lead to active *buying* of equities and to fragile market liquidity, albeit only contemporaneously. The fragility only shows through a sizeable jump in ILLIQ (18% on a one-standard deviation impulse). We find that the bid-ask spread jumps and depth drops, but these changes are economically negligible.[3]

Reassuringly, we find that these patterns are consistent with institutional trading. For 2009 through 2013, we use standard Abel Noser data on institutional order flow to redo the impulse-response analysis. We find statistically significant institutional selling of equities on VIX and VRP shocks and significant *buying* on ERV shocks.

In summary, we find evidence relating VIX shocks to flight to safety and to market fragility, but these are due to separate channels. Shocks to risk aversion (*VRP*) seem to trigger active re-allocation from equities to government bonds, without impairing market liquidity. Shocks to cash-flow risk (*ERV*), do not seem to trigger active re-allocation, but they do impair market liquidity, at least contemporaneously. The surprising finding is the *active buying* of equities that accompanies this market fragility.

This finding along with all other findings are rationalized in the last part of the manuscript by adding risk shocks to the model proposed by Vayanos and Wang (2012), which, itself, is an extension of Grossman and Stiglitz (1980). We add two types of risk shocks to those seeking liquidity. Liquidity demanders either become more risk averse (*VRP* channel), or they enter a market with elevated cash-flow risk (*ERV* channel). In the latter case, only the uninformed experience the increased uncertainty (i.e., the liquidity suppliers). This feature is in line with

[3]These findings suggest that standard, readily observable liquidity metrics such as spread and depth are imprecise measures for the cost of executing large orders. A better proxy for their transaction cost might be the price elasticity of net volume. This is in line with Hendershott and Menkveld (2014) who have an orthogonality result for the size of the bid-ask spread and the elasticity of (midquote) price elasticity to market-maker inventory, which both are endogenously derived in a dynamic inventory control model. Price elasticity in their model is the extent to which a market maker skews the bid and ask quote to mean-revert out of non-zero inventory. This might be the more relevant liquidity metric for liquidity demanders who trade large orders. This price elasticity might be what ILLIQ picks up in our analysis.

Grossman and Stiglitz (1980) where the uninformed bear additional uncertainty (simply because they know less).

Formal analysis of the two types of shocks in the model yields patterns that are consistent with the empirical findings. The results for the risk-aversion (*VRP*) channel are unsurprising. Investors who suddenly become more risk averse re-allocate risk to those who do not, hence the active selling of equities and buying of government bonds. Equity prices drop since the average investor becomes more risk-averse. Liquidity is unaffected, as the risk-aversion shocks are isomorphic to the endowment risk shocks that trigger trade in the core Grossman and Stiglitz (1980) model. These type of shocks do not affect liquidity which is offered perfectly competitively. Liquidity is costly in this model because of information asymmetry and the adverse-selection costs this imposes on uninformed liquidity suppliers. Risk-aversion or endowment risk shocks, however, do not change the level of information asymmetry.

The findings for the cash-flow risk (*ERV*) channel yield novel insights into the observed market dynamics. Active buying of the risky asset is an equilibrium result. The uninformed experience the additional cash-flow risk for the simple reason that they are *uninformed*. They understand that there is news and they realize that others have access to it. They therefore prefer to reduce their risky asset holdings. The informed observe the news and, therefore, bear less posterior risk. They sell on bad news, they buy on good news, but asymmetrically so, because, *on average*, they are buyers in equilibrium. The reason is that the cash-flow risk shock increases the wedge between the risk that the informed experience relative to the risk that the uninformed experience.

Not only does the cash-flow risk shock cause net buying of equities, it also makes the transfer costly because of increased information asymmetry. The uninformed liquidity suppliers experience higher adverse-selection costs and liquidity thus deteriorates. The cash-flow risk channel (*ERV*) therefore generates, on average, net buying by liquidity demanders on impaired liquidity supply, in line with our empirical findings.

Our findings that the root cause of risk shocks matters for how the market responds, add to a rapidly growing asset-pricing literature on the role of volatility. Ait-Sahalia et al. (2021), for example, motivate their model by quoting a New York Fed President who, in 2017, wondered: “You would think if uncertainty was high, you’d have a bit more volatility.” In their paper, they rationalize asset-price dynamics by introducing two disconnected stochastic processes: One that drives (realized) volatility and another that drives risk (aversion). Models in the same spirit are Liu et al. (2004), Drechsler (2013), and Brenner and Izhakian (2018). Similarly, in our analysis, the effects of heightened (experienced) uncertainty as measured by VIX shocks, depend on the underlying channel: Elevated risk aversion or elevated cash-flow risk.

The manuscript is organized as follows. Section 2 presents the data and the intraday VIX shock decomposition. Section 3 discusses the estimation of impulse-response functions, along with appropriate confidence intervals. Section 4 presents the main empirical findings: Market responses to VIX (component) impulses. Section 5 provides a deeper understanding of these findings by exploring a Grossmand-Stiglitz model. Section 6 concludes.

2 Data

2.1 NASDAQ message data

We collect message-level snapshots of the NASDAQ limit order book for four actively traded ETFs that provide exposure to different underlying baskets: S&P 500 (SPY), junk bonds (HYG), investment grade corporate bonds (LQD) and government bonds (TLT).[4] We retrieved and evaluate the entire available order book message history from July 1st, 2007 until April 7th, 2021 from data provider LOBSTER. Our sample contains a record for *each* message (submissions, adjustments, and cancellations of market and limit orders) and reconstructed snapshots of the complete order book for the first 50 levels.[5]

We restrict our analysis to order book activity during regular trading hours to avoid idiosyncrasies associated with opening and closing auctions. Therefore, we only consider messages between 10 a.m. and 3.30 p.m. EST (or 30 minutes after the opening auction and until 30 minutes before the closing auction if NASDAQ deviates from regular opening and closing hours, e.g., due to holidays). The entire dataset comprises more than 30 billion order book messages. We aggregate the order book messages for each ticker into the following six variables, measured at 5-minute intervals.

1. Initiator net volume (in million USD) which is the net of buyer and seller initiated shares transacted during the last 5-minute interval. We sign transactions as +1 if they are executed against a sell-side limit order and -1 if they are executed against a buy-side limit

[4]SPY tracks a basket of assets representing the S&P 500 index, HYG represents a basket of BBB to CCC rated corporate bonds with maturity less than 10 years and LQD represents a basket of more than 240 US corporate bonds with 5 to 20 years maturity which are A to BBB rated. TLT holds a 99% weight in US Treasury bonds with a maturity longer than 20 years

[5]We do not trim or winsorize any variables in our sample. After careful analysis we decided to remove two extreme and short-lived events from our analysis: A 10-minute episode during the Flash Crash period in the interval from May 6th, 2010 from 14:40 until 14:50 for which NASDAQ order book indicates unreasonably large order book imbalances and a 10-minute episode on April 29th, 2008 from 13:30 until 13:40 during which NASDAQ recorded a 1.5 Billion USD SPY buy market order which is more than 15 times the size of the *second-largest* observed buy order in the entire sample.

order. For execution against a hidden limit order, we impose the sign +1 if the transaction executes at a price that exceeds the last observed midquote and -1 if the transaction price is below the last observed midquote. To make the values comparable across assets, we multiply the aggregate net number of traded shares with the rolling 12-month average midquote computed for each ticker.

2. Return (in basis points) computed as $\log(p_{t,\tau}) - \log(p_{t,\tau-1})$ where t corresponds to the trading day and 5-minute timestamps are $\tau \in \{0, \ldots, 78\}$ which range from 09:30 a.m. ($\tau = 0$) until 4:00 p.m. ($\tau = 78$). $p_{t,\tau}$ is the last observed midquote on day t before timestamp τ.

3. Trading volume (in million USD) which is the cumulative trading volume during each 5-minute interval. We compute trading volume as the number of traded shares times the transaction price.

4. Bid-ask spread (in basis points) computed as the time-weighted average difference between the best prices quoted at the sell and buy side of the order book during each 5-minute interval. For every order book snapshot, we compute the bid-ask spread relative to the current midquote.

5. Depth (in million USD) measured as the number of posted shares in visible limit orders 5 basis points from the current best price on both sides of the order book. We take the time-weighted average depth during each interval to aggregate depth from message level into 5-minute intervals. To make the values comparable across assets, we multiply the number of available shares with the rolling 12-month average midquote computed for each ticker.

6. Amihud illiquidity measure, computed every five minutes as $ILLIQ_{t,\tau} := \frac{\left|\log(p_{t,\tau}) - \log(p_{t,\tau-1})\right|}{V_{t,\tau}}$. $ILLIQ_{t,\tau}$ corresponds to the absolute midquote log return divided by trading volume $V_{t,\tau}$ executed on NASDAQ (in million USD). High values indicate large price impacts per unit traded and are thus associated with illiquidity (Amihud, 2002). In our empirical analysis, we set $ILLIQ_{t,\tau}$ to missing for timestamps for which trading volume is zero.

Figure 1 illustrates the dynamics of the six variables for each ticker during the 14-year sample period. The figure shows the high dispersion of returns (measured, e.g., as the interquantile-range) during the global financial crisis and the COVID-19 market turbulence. In line with Angel et al. (2015) we confirm that quoted bid-ask spreads decreased considerably during the last years across all asset classes. At the same time, however, we document that depth also decreased for our selected ETFs. While Figure 1 illustrates this trend for depth measured

5 basis points around the current best price, Table AI in the Appendix provides additional summary statistics and indicates parallel trends deeper in the order book but also at the best level.

It should be noted that LOBSTER covers messages executed on NASDAQ only. Thus, trading volume $V_{t,\tau}$ is not a market-wide measure. Therefore, interpreting time trends for the ILLIQ time-series in our sample makes sense only under the assumption that NASDAQ market share has not changed over time. We do, however, expect a very high correlation between ILLIQ and a measure of illiquidity computed with market-wide trading volume at high frequencies.

2.2 Intraday VIX decomposition

Our starting point to investigate how a fear impulse ripples through the market is the CBOE Volatility Index (*VIX*), which is the implied volatility of the S&P 500 index. Besides its well-known role as a volatility index, VIX is often referred to as a fear gauge (Carr, 2017). The market prices of out-of-the-money puts and calls written on the S&P 500 index with maturity of one month determine the value of the VIX index. The construction of the VIX index value is such that the option-implied variance $IV_{t,\tau}$ of the S&P 500 index on trading day t and timestamp τ expressed in monthly percentages is $IV_{t,\tau} = \frac{\text{VIX}^2_{t,\tau}}{120{,}000}$.

In the asset pricing literature the difference between the *implied* variance as the risk-neutral expectation of the future return variation and the expected *realized* variance as its "physical" counterpart (i.e., computed under the actual physical probability measure) is of major importance. Defining $ERV_{t,\tau}$ as an estimate of the conditional expected realized variance of the S&P 500 index over the next month (i.e., until market closure 22 trading days ahead) and $IV_{t,\tau}$ as the option-implied variance of the S&P 500 index expressed in monthly percentages, we obtain

$$VRP_{t,\tau} := IV_{t,\tau} - ERV_{t,\tau} \tag{1}$$

as the so-called variance risk premium with respect to next month's return variation. Bollerslev et al. (2009, 2012, 2014) introduce this definition under the simplifying assumption that the realized variance follows a martingale process. Accordingly, in their definition, $ERV_{t,\tau}$ is replaced by the (observed) *ex post* realized variance through the previous month. This assumption, however, is challenged by Bekaert and Hoerova (2014) who exploit the predictability in realized variances and suggest Equation (1) on the basis of a prediction model for $ERV_{t,\tau}$.

Though Equation (1) is a common way to define the variance risk premium, the literature also suggests alternative definitions. A seminal contribution is Carr and Wu (2009) who

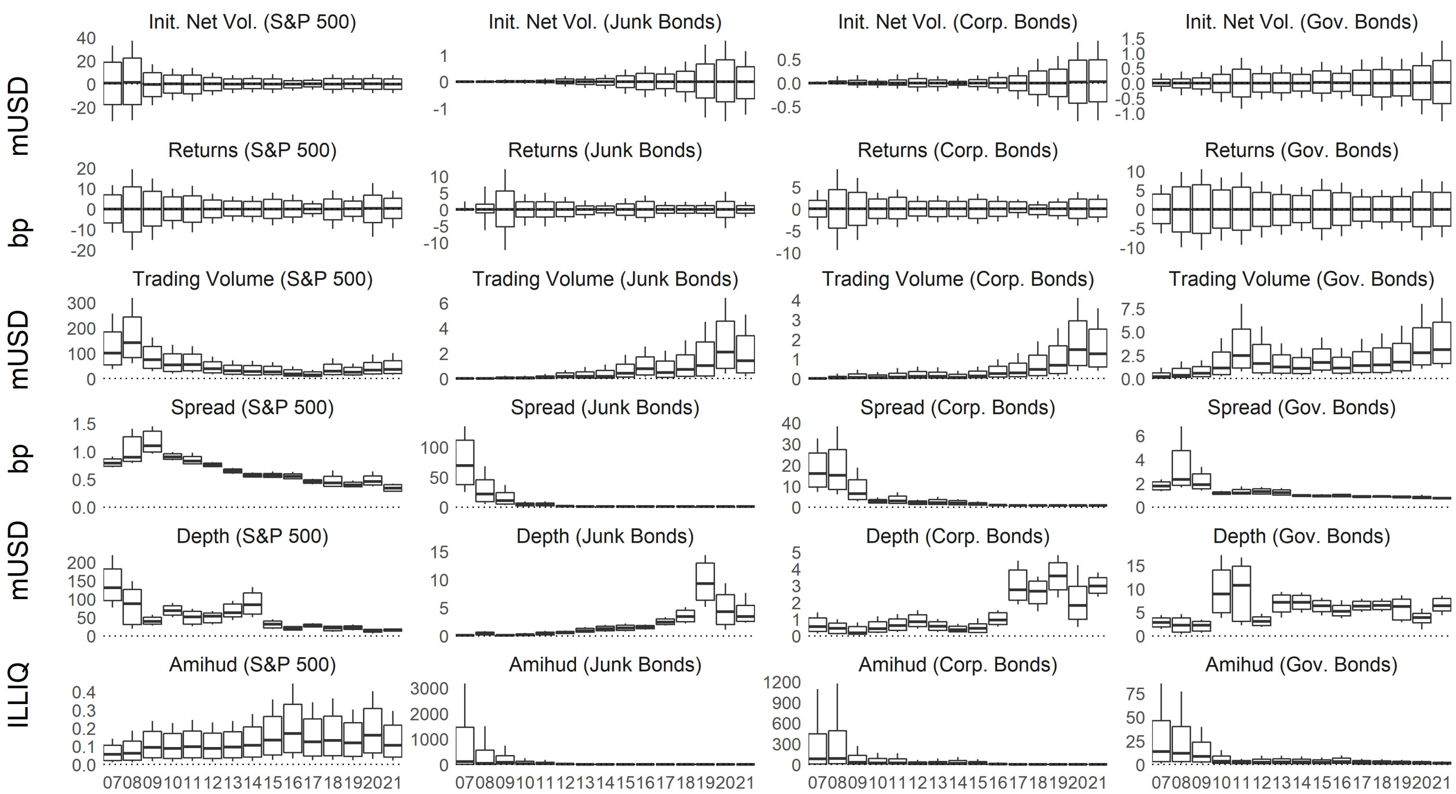

Figure 1: Summary statistics of the measured variables. *Initiator net volume* (in million USD), *return* (in basis points), *trading volume* (in million USD), *bid-ask spread* (in basis points), *depth* (in million USD) and the *Amihud* illiquidity measure. The assets correspond to ETFs which represent different baskets: *SPY* (S&P 500), *HYG* (Junk bonds), *LQD* (corporate bonds) and *TLT* (government bonds). We aggregate the 5-minute observations on an annual basis as box plots. The outer lines indicate the 5% and 95% quantiles, the boxes illustrate the first and third quartile as well as the median.

illustrate that the average variance risk premium corresponds to the sample average of the difference between the variance swap rate and the realized variance. According to this definition, the variance risk premium is typically *negative* and Equation (1) can be seen – strictly spoken – as an estimate of the *negative* variance risk premium. Alternative approaches define and estimate the variance risk premium under explicit stochastic volatility models, see, e.g., Bollerslev et al. (2011). Concepts of variance risk premia – though not necessarily explicitly defined – can also be found in earlier work, see, e.g., Rosenberg and Engle (2002), among others. Finally, some literature uses an alternative terminology. While we follow the terminology to call $VRP_{t,\tau}$ a "variance risk premium", Bekaert et al. (2013, 2021) associate $VRP_{t,\tau}$ with "risk aversion" (RA) and $ERV_{t,\tau}$ with "uncertainty" (UC). Accordingly, in their notation, the definition in Equation (1) reads as $RA_{t,\tau} = IV_{t,\tau} - UC_{t,\tau}$ but is conceptually identical.

Our approach extends the framework of Bekaert and Hoerova (2014) and Bekaert et al. (2021) by predicting the realized variance not only based on daily information, but also by utilizing intraday information. This makes our notation more complex, as we have to explicitly differentiate between intraday trading periods and overnight non-trading periods. We define the sequence of 5-minute timestamps $\tau \in \{0, \dots, 78\}$, which range from 09:30 a.m. ($\tau = 0$) until 4:00 p.m. ($\tau = 78$). We label the corresponding 5-minute returns as $r_{t,\tau} = \log(p_{t,\tau}) - \log(p_{t,\tau-1})$ for $\tau > 0$, where $p_{t,\tau}$ is the S&P 500 index value on the day t at timestamp τ. With a slight abuse of notation, we define $r_{t,0} = \log(p_{t,0}) - \log(p_{t-1,78})$ as the overnight return. We define

$$\widetilde{RV}_{t,\tau} := \sum_{k=0}^{\tau} r_{t,k}^2 \tag{2}$$

as the realized variance of the S&P 500 index, computed from the closure on day $t-1$ to the end of the τ-th 5-minute interval at day t (i.e., including the squared overnight return). Then, $RV_t := \widetilde{RV}_{t,78}$ defines the realized variance of the full trading day, measured from closure at day $t-1$ to closure on day t. Accordingly, the future realized variance, measured from the end of the τ-th 5-minute interval at day t to market closure d trading days ahead, is defined by

$$RV_{t,\tau}^{(d)} := \sum_{k=\tau+1}^{78} r_{t,k}^2 + \sum_{h=1}^{d} RV_{t+h} = \sum_{h=0}^{d} RV_{t+h} - \widetilde{RV}_{t,\tau}. \tag{3}$$

An empirically well-established and widely used model for the prediction of future realized variances is the heterogeneous autoregressive (HAR) model introduced by Corsi (2009). It builds on the high persistence of daily realized volatility, revealed by a slowly decaying autocorrelation function. The HAR model captures this behavior in a simple but empirically powerful way. Specifically, we model future realized variances based on averages of past realized variances, aggregated through different time horizons. A natural choice is to explain the future realized variance based on the last day's, last week's and last month's (average) realized variance. While Bekaert and Hoerova (2014) use the HAR framework based on daily data, we extend this framework to incorporate also intraday information. Accordingly, we model the log one-month-ahead realized variance, $RV^{(22)}_{t,\tau}$, measured from the end of the τ-th 5-minute interval at day t to market closure 22 trading days ahead, as

$$\begin{aligned}\log\left(RV^{(22)}_{t,\tau}\right) = c_\tau + \beta_\tau \log\left(RV^{(21)}_{t-22,0} + \widetilde{RV}_{t,\tau}\right) + \gamma_\tau \log\left(RV^{(4)}_{t-5,0} + \widetilde{RV}_{t,\tau}\right) \\ + \delta_\tau \log\left(\widetilde{RV}_{t,\tau}\right) + \varepsilon_{t,\tau},\end{aligned} \tag{4}$$

where $\varepsilon_{t,\tau}$ is zero mean white noise and $\left(RV^{(d-1)}_{t-d,0} + \widetilde{RV}_{t,\tau}\right)$ is the sum of the realized variance measured from market opening d trading days ago until the closure on the previous day $\left(RV^{(d-1)}_{t-d,0}\right)$ and the realized variance measured from closure on the previous day until the most recent observation on day t in intraday interval τ $\left(\widetilde{RV}_{t,\tau}\right)$. For the special case $\tau = 78$, these components collapse to $RV^{(d-1)}_{t-d,0} + RV_t = RV^{(d)}_{t-d,0}$, corresponding to the d-day realized variance measured from the opening d days ago until the closure on the current day. Likewise, $\widetilde{RV}_{t,78} = RV_t$ collapses to the realized variance measured from previous day's to current day's closure. In this case, Equation (4) resembles the initial HAR model by Corsi (2009) including realized variances of the most recent day, the previous 5 days and the previous 22 days and nests the daily regression setup of Bekaert and Hoerova (2014).

We use this framework as a natural starting point for predicting future realized variances using information up to day t, timestamp τ. An obvious extension is to incorporate not only lagged realized variances (and squared overnight returns), but also information from other trading variables and from other assets. In our sample we find that expanding the relevant set of conditioning information to contemporaneous *VIX* levels and limit order book data does only marginally increase the predictive performance leaving Equation (4) as a parsimonious and powerful benchmark.

Note that the regression coefficients in Equation (4) depend on the timestamp τ, i.e., the predictive power of past realized variances differs depending on the intraday period. Intuitively, we expect that the importance of $\widetilde{RV}_{t,\tau}$ increases, as the trading day progresses. In order to avoid imposing assumptions on the intraday evolution of $c_\tau, \beta_\tau, \gamma_\tau$, and δ_τ, we estimate the parameters in Equation (4) for each value of $\tau \in \{1, \dots, 78\}$, yielding 78 individual regressions. To avoid look-ahead biases, we conduct rolling estimation windows with estimation length of 12 months. For that purpose, we extract 5-minute S&P 500 index values and 5-minute VIX index levels from the data provider *pitrading*. Our sample starts already in July 2006 such that we obtain estimates of the predictive regression for the entire period for which order book information from LOBSTER is available.

Estimation of the parameters in Equation (4) for $\tau \in \{1, \dots, 78\}$ by least squares yields the sequence $\{\hat{c}_\tau, \hat{\beta}_\tau, \hat{\gamma}_\tau, \hat{\delta}_\tau\}$ and thus

$$\widehat{E}_{t,\tau}\left(RV_{t,\tau}^{(22)}\right) = \exp\left(\hat{c}_\tau + \hat{\beta}_\tau \log\left(RV_{t-22,0}^{(21)} + \widetilde{RV}_{t,\tau}\right) + \hat{\gamma}_\tau \log\left(RV_{t-5,0}^{(4)} + \widetilde{RV}_{t,\tau}\right) + \hat{\delta}_\tau \log\left(\widetilde{RV}_{t,\tau}\right)\right). \tag{5}$$

Accordingly, for each day t and timestamp τ we obtain the estimated variance risk premium $\widehat{VRP}_{t,\tau}$ as

$$\widehat{VRP}_{t,\tau} = IV_{t,\tau} - \widehat{E}_{t,\tau}\left(RV_{t,\tau}^{(22)}\right). \tag{6}$$

Figure 2 illustrates the time series of the implied variance $IV_{t,\tau}$ and the realized variance $RV_{t,\tau}^{(22)}$ for the next 22 days. Note, that in line with Bollerslev et al. (2015), the average implied variance exceeds the average realized variance, which suggests that the unconditional mean of the variance risk premium is positive. The figure reveals two extreme periods of elevated variance-risk premia during the last 14 years: the global financial crisis and the market turbulences related to the outbreak of the COVID-19 pandemic in March 2020.

The figure largely resembles the findings of Bekaert et al. (2021) and illustrates persistent variations of the variance risk premium during volatile market periods. In line with Bekaert et al. (2021) we find that $\widehat{VRP}_{t,\tau}$ is positive after large shocks for a while but tends to zero during periods of minor shocks. This suggests that the representative investor is risk averse in periods following shocks, but close to risk-neutral if no further large shocks hit the market for an extended period. The two components, *VRP* and *ERV* are close to orthogonal at a five-minute frequency.[6]

The regression results itself indicate the relevance of intraday data even for long run forecasts of the realized variance. Figure A1 in the Appendix illustrates the goodness-of-fit and the estimated regression coefficients of the predictive regression in Equation (4). We find that the average full-sample adjusted R^2 of the predictive regression in Equation (4) is 35%. Omitting $\widetilde{RV}_{t,\tau}$ in Equation (4) and setting $\delta_\tau = 0$ yields a smaller average adjusted R^2 of 33%. The

[6]The sample correlation between the two components is negative in the data, but we believe this is spurious and due to imperfect estimation of the *ERV* change. Given that we compute the *VRP* component as the residual component, a positive measurement error in *ERV* mechanically becomes a negative measurement error in VRP.

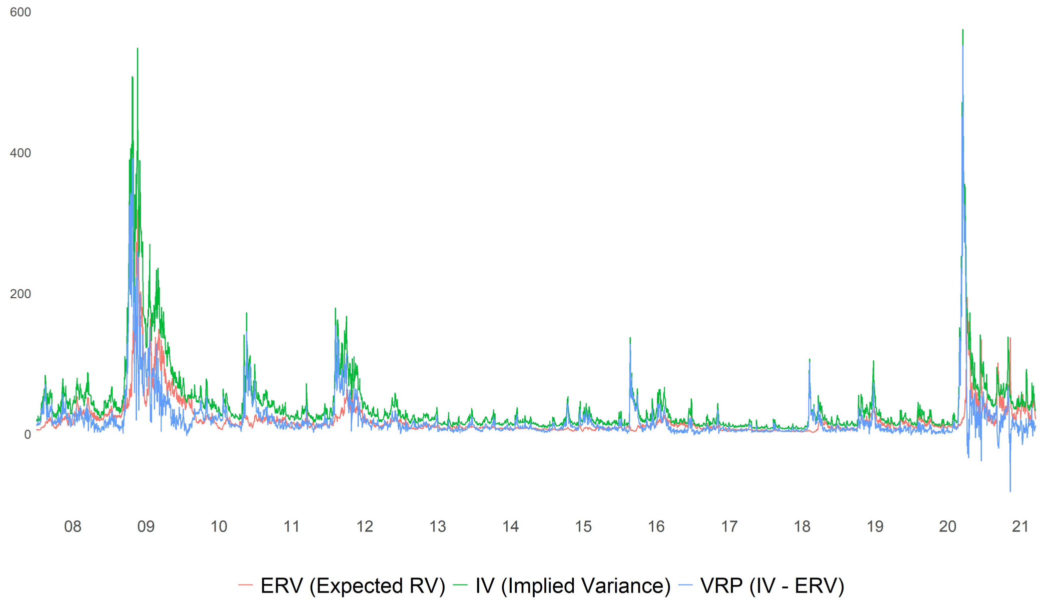

Figure 2: Time-series of the implied variance and the expected realized variance time series (all in monthly percentages). To compute the implied variance (*IV*), we convert VIX index values as $VIX^2_{t,\tau}/120,000$. *ERV* is the predicted realized variance $E_{t,\tau}(RV_{t,\tau}(22))$ as of Equation (4) and *VRP* is the estimated variance risk premium $(IV - ERV)$ where the realized future variance $RV^{(22)}_{t,\tau}$ is the sum of squared 5-minute S&P 500 returns from the current point in time until the market close 22 trading days ahead.

upwards slope for our benchmark model indicates that as the trading day progresses, future realized variances can be explained considerably better than at the beginning of the trading day. At the same time, ignoring intraday information by omitting $\widetilde{RV}_{t,\tau}$ in the regression indicates that as the trading day progresses, the predictive performance for future realized variances becomes worse, presumably because $RV^{(21)}_{t-22,0}$ and $RV^{(4)}_{t-5,0}$ are based on information that becomes more and more outdated.

The sequence of estimated regression coefficients indicates that $RV^{(4)}_{t-5,0}$ plays the most important role to predict future realized variance. It is important to note, however, that $\hat{\delta}_\tau$ is significantly different from zero for each regression specification. We thus find that intraday information receives substantially higher weights towards the end of the trading day relative to the static model.

3 Quantifying impulse responses

3.1 Local projections

Our aim is to quantify the responses of the time series in our sample to an implied variance (IV) shock or its components, i.e., the variance risk premium VRP (related to risk aversion) or the expected realized variance *ERV* (related to future cash flow risks). Denote the $(N \times 1)$ vector of observations at time point τ by $\boldsymbol{y}_\tau = (y_{\tau,1}, \ldots, y_{\tau,N})'$. We assume that $\boldsymbol{y}_\tau$ follows a vector autoregressive (VAR) model of the form

$$\boldsymbol{y}_\tau = \sum_{j=1}^{p} \boldsymbol{A}_j \boldsymbol{y}_{\tau-j} + \boldsymbol{u}_\tau, \tag{7}$$

where $\boldsymbol{A}_j$ are $(N \times N)$ coefficient matrices and $\boldsymbol{u}_\tau$ are $(N \times 1)$ vectors of white noise variables with variance-covariance matrix $\boldsymbol{\Sigma}_u$. Impulse response functions (IRFs) measure the response of the variable $y_{\tau+h,i}$ to a shock $\boldsymbol{d}$ of the error term vector $\boldsymbol{u}_\tau$ in period τ. By defining $\mathcal{F}_\tau := \{\boldsymbol{y}_\tau, \ldots, \boldsymbol{y}_1\}$, the common definition of an IRF is the difference between the conditional expectations $E\left(y_{\tau+h,i} | \boldsymbol{u}_\tau = \boldsymbol{d}, \mathcal{F}_{\tau-1}\right)$ and $E\left(y_{\tau+h,i} | \boldsymbol{u}_\tau = \boldsymbol{0}_N, \mathcal{F}_{\tau-1}\right)$, where $\boldsymbol{0}_N$ denotes a $(N \times 1)$ vector of zeros. In case of VAR models, this definition is equivalent to

$$\mathrm{ir}_i\left(\boldsymbol{u}_\tau, h, \boldsymbol{d}\right) := E\left(y_{\tau+h,i} | \boldsymbol{u}_\tau = \boldsymbol{d}, \mathcal{F}_{\tau-1}\right) - E\left(y_{\tau+h,i} | \mathcal{F}_{\tau-1}\right), \tag{8}$$

where in the latter term the variables $\boldsymbol{u}_\tau$ are integrated out. This concept is referred to as *generalized* impulse response function according to Koop et al. (1996).

Denote $\boldsymbol{e}_i$ as the $(N \times 1)$ selection vector with unity as i-th element and zeros otherwise. In the given VAR model according to Equation (7), the IRF can be obtained from the corresponding moving average representation $\boldsymbol{y}_{\tau+h} = \sum_{l=0}^{\infty} \boldsymbol{\Phi}_l \boldsymbol{u}_{\tau+h-l}$, where $\boldsymbol{\Phi}_0 = \boldsymbol{I}_N$ is the $(N \times N)$ identity matrix and $\boldsymbol{\Phi}_l$ are the MA coefficient matrices corresponding to $\boldsymbol{\Phi}_l = \partial \boldsymbol{y}_{\tau+l} / \partial \boldsymbol{u}'_\tau$. Then, the IRF is obtained by

$$\mathrm{ir}_i\left(\boldsymbol{u}_\tau, h, \boldsymbol{d}\right) = \boldsymbol{e}'_i \boldsymbol{\Phi}_h \boldsymbol{d}. \tag{9}$$

Estimating the IRF requires backing out estimates of $\boldsymbol{\Phi}_l$ from the estimates of underlying VAR coefficients $\boldsymbol{A}_j$, $j = 1, \ldots, p$. As a result, estimates are prone to estimation errors and sensitive to the choice of the underlying VAR model.

Estimating $\mathrm{ir}_i\left(\boldsymbol{u}_\tau, h, \boldsymbol{d}\right)$ in a 'direct' way by local projections as proposed by Jorda (2005) avoids these difficulties. To illustrate the idea of local projections, we re-formulate Equation (7) for $y_{\tau+h,i}$ and express the process – by backward substitution – in terms of $\boldsymbol{y}_\tau, \boldsymbol{y}_{\tau-1}, \ldots, \boldsymbol{y}_{\tau-(p-1)}$:

$$y_{\tau+h,i} = \boldsymbol{\beta}_i(\boldsymbol{A}, h)' \boldsymbol{y}_\tau + \sum_{l=1}^{p-1} \boldsymbol{\delta}_{l,i}(\boldsymbol{A}, h)' \boldsymbol{y}_{\tau-l} + \xi_{\tau,i}. \tag{10}$$

Here, $\boldsymbol{\beta}_i(\boldsymbol{A}, h)$ denotes the $(N \times 1)$ vector of local projection coefficients, and corresponds to a function of the VAR coefficient matrices $\boldsymbol{A}_1, \ldots, \boldsymbol{A}_p$. Likewise, $\boldsymbol{\delta}_{l,i}(\boldsymbol{A}, h)$ is a $(N \times 1)$ vector of coefficients associated with $\boldsymbol{y}_{\tau-l}$, $l \geq 1$. Finally, $\xi_{\tau,i} = \sum_{l=1}^{h} \boldsymbol{\beta}_i(\boldsymbol{A}, h-l)'\boldsymbol{u}_{\tau+l}$ is the model-implied h-step-ahead forecasting error. For example, in the special case of a VAR(1) model, we have $\boldsymbol{\delta}_{l,i}(\boldsymbol{A}, h) = \boldsymbol{0}$ for $l \geq 1$ and $\boldsymbol{\beta}_i(\boldsymbol{A}, h) = (\boldsymbol{A}_1^h)'\boldsymbol{e}_i$, corresponding to the (transposed) i-th row of the matrix $\boldsymbol{A}_1^h$.

Local projection coefficients $\boldsymbol{\beta}_i(\boldsymbol{A}, h)$ correspond to the derivatives $\partial \boldsymbol{y}_{\tau+h,i}/\partial \boldsymbol{y}_\tau = \partial \boldsymbol{y}_{\tau+h,i}/\partial \boldsymbol{u}_\tau = (\partial \boldsymbol{y}_{\tau+h}/\partial \boldsymbol{u}_\tau')'\boldsymbol{e}_i$ and thus we have $\boldsymbol{\beta}_i(\boldsymbol{A}, h) = \boldsymbol{\Phi}_h'\boldsymbol{e}_i$. Consequently, an alternative formulation of $\mathrm{ir}_i\left(\boldsymbol{u}_\tau, h, \boldsymbol{d}\right) = \boldsymbol{e}_i'\boldsymbol{\Phi}_h\boldsymbol{d}$ is

$$\mathrm{ir}_i\left(\boldsymbol{u}_\tau, h, \boldsymbol{d}\right) = \boldsymbol{\beta}_i(\boldsymbol{A}, h)'\boldsymbol{d}. \tag{11}$$

It is straightforward to estimate the local projection coefficients $\boldsymbol{\beta}_i(\boldsymbol{A}, h)$ by means of a linear regression of $y_{\tau+h,i}$ on $\boldsymbol{x}_\tau := (\boldsymbol{y}_\tau', \boldsymbol{y}_{\tau-1}', \ldots, \boldsymbol{y}_{\tau-p-1}')'$, yielding the OLS estimates

$$\begin{pmatrix} \hat{\boldsymbol{\beta}}_i(h) \\ \hat{\boldsymbol{\gamma}}_i(h) \end{pmatrix} = \left(\sum_{\tau=1}^{T-h} \boldsymbol{x}_\tau \boldsymbol{x}_\tau' \right)^{-1} \sum_{\tau=1}^{T-h} \boldsymbol{x}_\tau y_{\tau+h,i}, \tag{12}$$

where $\hat{\boldsymbol{\beta}}_i(h)$ is the $(N \times 1)$ vector of OLS coefficients associated with $\boldsymbol{y}_\tau$. As shown by Montiel Olea and Plagborg-Møller (2021), $\hat{\boldsymbol{\beta}}_i(h)$ is a consistent estimator of $\boldsymbol{\beta}_i(\boldsymbol{A}, h)$, and thus $\widehat{ir}_i\left(\boldsymbol{u}_\tau, j, \boldsymbol{d}\right) = \hat{\boldsymbol{\beta}}_i(h)'\boldsymbol{d}$ is a consistent estimator of the impulse response function $\mathrm{ir}_i(\boldsymbol{u}_\tau, h, \boldsymbol{d})$.

Likewise, we obtain estimates of the cumulative impulse response function from

$$\widehat{cir}_i(\boldsymbol{u}_\tau, h, \boldsymbol{d}) = \sum_{j=0}^{h} \widehat{ir}_i(\boldsymbol{u}_\tau, j, \boldsymbol{d}) = \sum_{j=1}^{h} \hat{\boldsymbol{\beta}}_i(j)'\boldsymbol{d}, \tag{13}$$

since $\hat{\boldsymbol{\beta}}_i(0) = \boldsymbol{I}_N$.

3.2 Lag-augmentation

While the least square estimator $\hat{\boldsymbol{\beta}}_i(h)$ is consistent, it is not easy to compute standard errors since the residuals $\hat{\xi}_{\tau,i}$ based on Equation (12) are serially correlated. This requires the construction of a heteroscedasticity and autocorrelation consistent (HAC) estimator of the error covariance matrix, which is not straightforward and renders inference challenging.

As an alternative, Montiel Olea and Plagborg-Møller (2021) propose estimating $\boldsymbol{\beta}_i(\boldsymbol{A}, h)$ by lag augmentation, which keeps the estimator consistent but removes the serial dependence in the residuals. The idea of lag augmentation is to augment the regressors $\boldsymbol{x}_\tau$ by one additional lag, $\boldsymbol{y}_{\tau-p}$, which serves as an additional control variable.

Hence, in the lag-augmented regression, we regress $y_{\tau+h,i}$ on $\tilde{\boldsymbol{x}}_\tau := (\boldsymbol{y}_\tau', \boldsymbol{y}_{\tau-1}', \ldots, \boldsymbol{y}_{\tau-p}')'$ yielding

$$\begin{pmatrix} \hat{\boldsymbol{\beta}}_i^a(h) \\ \hat{\boldsymbol{\gamma}}_i^a(h) \end{pmatrix} = \left(\sum_{\tau=1}^{T-h} \tilde{\boldsymbol{x}}_\tau \tilde{\boldsymbol{x}}_\tau' \right)^{-1} \sum_{\tau=1}^{T-h} \tilde{\boldsymbol{x}}_\tau y_{\tau+h,i}, \tag{14}$$

where $\hat{\boldsymbol{\beta}}_i^a(h)$ is of dimension $(N \times 1)$. Montiel Olea and Plagborg-Møller (2021) show that $\hat{\boldsymbol{\beta}}_i^a(h)'\boldsymbol{d}$ is also a consistent estimator for $\mathrm{ir}_i(\boldsymbol{u}_\tau, h, \boldsymbol{d})$, while the residuals resulting from this regression are serially uncorrelated. Thus, standard errors of $\hat{\boldsymbol{\beta}}_i^a(h)$ can be computed using the Eicker-Huber-White heteroscedasticity-robust covariance estimator without the need of controlling for serial correlation.

3.3 Choice of the shock size

Contemporaneous correlations of the errors $\boldsymbol{u}_\tau$, i.e., a non-diagonal covariance matrix $\boldsymbol{\Sigma}_u$, render it impossible to attribute a shock exclusively to a single variable. A traditional solution, as proposed by Sims (1980), is to orthogonalize the errors based on a Cholesky decomposition of $\boldsymbol{\Sigma}_u$. The orthogonalized errors then depend recursively on the original errors, which makes the approach sensitive to the ordering of the variables.

To overcome the need of imposing an (often arbitrary) ordering of the variables, Pesaran and Shin (1998) and Koop et al. (1996) make use of the definition of a IRF as of Equation (8) and the fact that under the assumption of multivariate normality of $\boldsymbol{u}_\tau$, it follows that $\boldsymbol{d} = E(\boldsymbol{u}_\tau | u_{\tau,j} = \delta) = \boldsymbol{\Sigma}_{\boldsymbol{u}} \boldsymbol{e}_j \sigma_{jj}^{-1} \delta$, where σ_{jj} is the j-th diagonal element of $\boldsymbol{\Sigma}_{\boldsymbol{u}}$ and $\delta \neq 0$ denotes the shock in element j. Intuitively, a shock on the j-th error with size δ implies instantaneous adjustments in all other errors due to contemporaneous correlations as reflected by $\boldsymbol{\Sigma}_{\boldsymbol{u}}$. This yields IRFs which are insensitive to the initial ordering of the variables.

By choosing δ as a one-standard-deviation shock, $\delta = \sqrt{\sigma}_{jj}$, we therefore obtain

$$\boldsymbol{d} = E\left(\boldsymbol{u}_\tau | u_{\tau,j} = \sqrt{\sigma}_{jj}\right) = \boldsymbol{\Sigma}_{\boldsymbol{u}} \boldsymbol{e}_j \sigma_{jj}^{-1/2}. \tag{15}$$

Given a consistent estimate $\hat{\boldsymbol{\Sigma}}_{\boldsymbol{u}}$, the IRF is then estimated as

$$\widehat{ir}_i\left(\boldsymbol{u}_\tau, h, \boldsymbol{d}\right) = \hat{\boldsymbol{\beta}}_i^a(h)' \hat{\boldsymbol{\Sigma}}_{\boldsymbol{u}} \boldsymbol{e}_j \hat{\sigma}_{jj}^{-1/2}. \tag{16}$$

We implement this approach in three steps. First, we determine the lag length of the underlying VAR process using the AIC criterion. Then, $\hat{\boldsymbol{\beta}}_i^a(h)$ results from corresponding lag-augmented local projections as of Equation (14). Finally, we obtain $\hat{\boldsymbol{\Sigma}}_{\boldsymbol{u}}$ from maximum likelihood estimates based on the residuals of a VAR(p) process.

3.4 Standard errors

We show in the Appendix that for $T \to \infty$

$$\sqrt{T}\left(\widehat{\mathrm{ir}}_i(\boldsymbol{u}_\tau, h, \boldsymbol{d}) - \mathrm{ir}_i(\boldsymbol{u}_\tau, h, \boldsymbol{d})\right) \overset{a}{\sim} N\left(0, \boldsymbol{d}' AV[\hat{\boldsymbol{\beta}}_i^a(h)]\boldsymbol{d} + \frac{2}{\sigma_{jj}} \boldsymbol{U}\boldsymbol{P}(\boldsymbol{\Sigma}_{\boldsymbol{u}} \otimes \boldsymbol{\Sigma}_{\boldsymbol{u}})\boldsymbol{U}'\right), \tag{17}$$

where $AV[\hat{\boldsymbol{\beta}}_i^a(h)]$ is the asymptotic variance of $\sqrt{T}\hat{\boldsymbol{\beta}}_i^a(h)$, $\boldsymbol{e}_j$ denotes an $(N \times 1)$ selection vector, $\boldsymbol{U} = \left(\boldsymbol{e}_j' \otimes \boldsymbol{\beta}_i^a(h)'\right) - 1/2\sigma_{jj}^{-1/2}\mathrm{ir}_i(\boldsymbol{u}_\tau, h, \boldsymbol{d})\left(\boldsymbol{e}_j' \otimes \boldsymbol{e}_j'\right)$, and $\boldsymbol{P} = \boldsymbol{D}_N(\boldsymbol{D}_N'\boldsymbol{D}_N)^{-1}\boldsymbol{D}_N'$ is the $\left(N^2 \times N^2\right)$ projection matrix based on the duplication matrix $\boldsymbol{D}_N$.

Then, using the (Eicker-Huber-White heteroscedasticity-robust) estimates $\hat{V}[\hat{\boldsymbol{\beta}}_i^a(h)]$ resulting from the local projections and the maximum likelihood estimates $\hat{\boldsymbol{\Sigma}}_{\boldsymbol{u}}$ yields the standard errors for $\widehat{\mathrm{ir}}_i(\boldsymbol{u}_\tau, h, \boldsymbol{d})$ given by

$$\mathrm{SE}(\widehat{\mathrm{ir}}_i(\boldsymbol{u}_\tau, h, \boldsymbol{d})) = \hat{V}(\widehat{\mathrm{ir}}_i(\boldsymbol{u}_\tau, h, \boldsymbol{d}))^{1/2} = \left(T^{-1}\hat{\boldsymbol{d}}'\hat{V}[\hat{\boldsymbol{\beta}}_i^a(h)]\hat{\boldsymbol{d}} + \frac{2}{\hat{\sigma}_{jj}}\hat{\boldsymbol{U}}\boldsymbol{P}\left(\hat{\boldsymbol{\Sigma}}_{\boldsymbol{u}} \otimes \hat{\boldsymbol{\Sigma}}_{\boldsymbol{u}}\right)\hat{\boldsymbol{U}}'\right)^{1/2}, \tag{18}$$

where $\hat{\boldsymbol{d}} = \hat{\boldsymbol{\Sigma}}_{\boldsymbol{u}}\boldsymbol{e}_j\hat{\sigma}_{jj}^{-1/2}$, and $\hat{\boldsymbol{U}} = \left(\boldsymbol{e}_j' \otimes \hat{\boldsymbol{\beta}}_i^a(h)'\right) - \frac{1}{2}\hat{\sigma}_{jj}^{-1/2}\widehat{\mathrm{ir}}_i(\boldsymbol{u}_\tau, h, \boldsymbol{d})\left(\boldsymbol{e}_j' \otimes \boldsymbol{e}_j'\right)$.

Likewise, as we also show in the Appendix, standard errors of the estimated cumulative impulse response function $\widehat{cir}_i(\boldsymbol{u}_\tau, h, \boldsymbol{d})$ can be computed by Equation (18) with $\hat{\boldsymbol{\beta}}_i^{a(h)}$ replaced by $\sum_{k=1}^{h}\hat{\boldsymbol{\beta}}_i^{a(h)}$ and $\hat{V}[\hat{\boldsymbol{\beta}}_i^{a(h)}]$ replaced by $\sum_{k=1}^{h}\hat{V}[\hat{\boldsymbol{\beta}}_i^{a(h)}]$.

4 Market responses to a VIX impulse

In this section we estimate IRFs to quantify market responses to an implied variance (*IV*) shock. Then, to understand the driving channels of the responses we separately analyze responses to a shock in the variance risk premium (*VRP*) or the expected realized variance (*ERV*).

The response variables are always the time-series of 5-minute observations of the six aggregated order book variables (initiator net volume, return, trading volume, bid-ask spread, depth and ILLIQ) for each of the four ETFs (which track S&P 500, Junk Bonds, Corporate Bonds, and Government Bonds).

To characterize responses, we estimate IRFs based on Equation (16). To compute confidence intervals, we rely on the standard errors of $\widehat{ir}_i(\boldsymbol{u}_\tau, h, \boldsymbol{d})$ and $\widehat{cir}_i(\boldsymbol{u}_\tau, h, \boldsymbol{d})$ in Equation (18). When lagging variables, we only include observations from the same trading day such that we exclude overnight effects from the analysis.

We always report the estimated cumulative impulse response functions for initiator net volume (in million USD) and return (in basis points). We report impulse response functions for trading volume and depth (all in million USD), bid-ask spreads (in basis points) and the Amihud (ILLIQ) measure.

4.1 Responses to a VIX shock

Figure 3 illustrates the estimated instantaneous (0 minute), 20 minute, 40 minute and 60 minute responses to a positive shock in implied variance *(IV) changes*.[7] The estimated IRFs therefore reflect how a risk shock, materialized as a sudden *VIX* increase, ripples through financial markets at different frequencies. Our main insights as follows:

Strong initiated sell-side volume for risky assets. Investors initiate net selling of the S&P 500, Junk Bonds and Corporate Bonds as a response to an *IV* shock. Within the first 5 minutes after the *IV* shock, net selling of S&P 500 worth more than USD 3 million shock hits the market. While the sell-off of the risky assets starts as soon as the *IV* shock hits, negative cumulative net initiated increases within the hour by almost 40%. Asset prices react, even substantially faster than initiated selling to the predictable portfolio re-balancing triggered by the *IV* shock. The second row of Figure 3 indicates that the immediate price impact of the initiated selling in the S&P 500 is about six basis points. The effects are economically meaningful: The instantaneous initiated sell side volume in the S&P 500 corresponds to a negative 0.25 standard deviation response. Prices of Junk Bonds and Government Bonds also decline, consistent with the initiated selling of risky asset. The negative return response for the S&P 500 is larger than 0.6 standard deviations. The response functions indicate that the immediate response to the unpredictable shock in *IV* is stronger than the long-run responses. This finding is in line with market makers anticipating the predictable orderflow and thus reflect a liquidity premium for immediate responses to a sudden *IV* shock (e.g., Capponi et al., 2021). More specifically, the return effect of the shock declines by about 20% in the subsequent hour. The effect is present only to a limited extent for Junk and Corporate Bonds.

Flight to safe government bonds. The *IV* shock triggers net initiated buying of safe government bonds. We interpret the response as a re-allocation from risky assets to government bonds in the sense of a flight to safety. The initiated net buying of government bonds amplifies

[7] We do not report the response of (cumulative) *IV* changes in the main figures. *IV* shocks are persistent, in the sense that a one standard deviation *IV* shift triggers a further 8% increase during the next 20 minutes and then slowly decays again.

as the *IV* shock triggers continued buying of government bonds within the hour. Prices for Government Bonds instantaneously increase by 1.2 basis points and reflect the sudden demand shock and increase.

Liquidity remains stable after *IV* shock. Liquidity responses to an *IV* shock are of minor economic magnitudes. Rows three to six of Figure 3 illustrate the responses in terms of bid-ask spread, depth and ILLIQ to a sudden *IV* shock. While trading volume across all asset classes increases significantly, both instantaneously and within the hour, bid-ask spreads, order book depth and the ILLIQ measure responses are of minor economic magnitudes. The instantaneous responses indicate that the bid-ask spread increases slightly for S&P 500 in response to an *IV* shock but remain unchanged or even narrow slightly for the remaining assets. Order book depth decreases across all asset classes. Surprisingly, we find that illiquidity for the S&P 500 decreases in response to an *IV* shock, while it increases for Corporate Bonds and remains constant for Government Bonds and Junk Bonds. Within the hour, order book depth drops across all assets that exhibit initiated net selling and bid-ask spreads widen.

Our IRFs thus reveal that investors fly to safety in times of elevated risk. An *IV* shock triggers fast net selling of risky assets and simultaneous initiated net buying of government bonds. The responses reveal that such portfolio re-allocation at the high-frequency level does not to trigger liquidity spirals immediately as a response. Liquidity provisioning remains largely unchanged and thus absorbs the demand for fast re-allocation.

4.2 Delineating the VIX impulse responses

As outlined in Section 2.2, a shock of *IV* indicates an increase in volatility under the risk-neutral measure but does not reveal whether heightened future cash flow risk or an increase in the variance risk premium causes the change. We use our intraday decomposition of the implied variance from Equation (6) as the sum of expected realized volatility (*ERV*, related to cash flow risks) and the variance risk premium (*VRP*, related to risk aversion)

$$IV_{t,\tau} = \widehat{E}_{t,\tau}\left(RV_{t,\tau}^{(22)}\right) + \widehat{VRP}_{t,\tau} \tag{19}$$

and shock the two components individually.

For that purpose, we include the 24 time series from our limit order book sample together with changes in $\widehat{E}_{t,\tau}\left(RV_{t,\tau}^{(22)}\right)$ and changes in $\widehat{VRP}_{t,\tau}$ into our IRF estimations. As in Section 4.1, we compute the responses of the limit order book variables. Figure 4 illustrates the responses

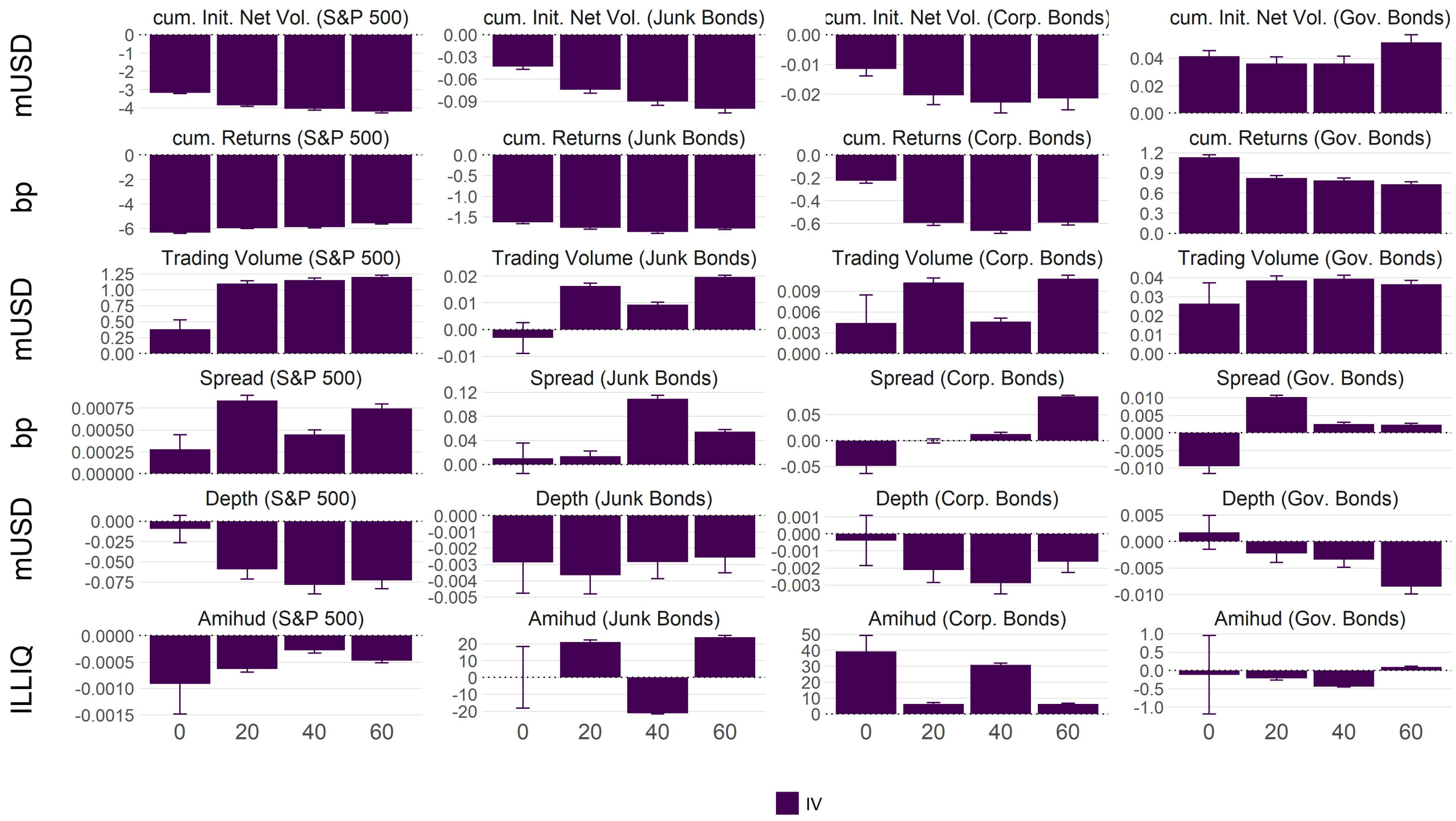

Figure 3: Estimated impulse response functions based on the entire sample (July 1st, 2007 until April 7th, 2021). We shock *IV* changes by one positive standard deviation. *Returns* and *initiator net volume* responses denote *cumulative* responses, whereas we report impulse responses for *trading volume*, *depth*, *bid-ask spread* and the *Amihud (ILLIQ) measure*. We report *Return* and *bid-ask spread* responses in basis points and denote all remaining variables in million USD. *Horizon* denotes the instantaneous (0 minute), 20 minute, 40 minute and 60 minute responses. The error bars illustrate 95% confidence intervals.

to the individual shocks. The shock sizes are always a positive standard deviation, which corresponds either to an increase in the variance risk premium (*VRP*) or the expected realized variance (*ERV*). To make the responses comparable, we include the purple bar (*IV*) which corresponds to the responses based on imposing a positive shock on *IV* already presented in Figure 3.

4.2.1 Responses to an *VRP* shock

The responses to an *VRP* shock are unsurprising and mirror the response to a *VIX* shock. Thus, a variance-risk premium increase triggers a flight to safety on largely unchanged liquidity: In a response to a *VRP* shock, markets respond with net selling of the S&P 500, Corporate Bonds and Junk Bonds and simultaneously net buying of government bonds. Prices adjust in line with net initiated trading direction: As a response to *VRP* shock, equity market valuation drops by about 4 basis points (0.6 standard deviations) and government bonds appreciate by about 1 basis point (0.2 standard deviations) in value.

Liquidity remains largely unchanged and is in line with the responses to an *IV* shock. Depth slightly deteriorates across all asset classes and spreads widen but only at small magnitudes.

4.2.2 Responses to an *ERV* shock

Initiated buying of equity. A shock in the *ERV* triggers *positive* initiator net volume for S&P 500. Thus, after the expected realized variance increases, liquidity demanders start buying of the risky assets. Such buying is in stark contrast to the flight to safety dynamics in response to an *VRP* shock: Liquidity demanders seem to become net buyers of risky assets after the *ERV* shock arrives. The responses indicate initiated net selling of Junk Bonds and less clear responses in Corporate Bonds.

Liquidity deteriorates. In response to an *ERV* shock, ILLIQ increases substantially, which suggests higher price impact on volume. Thus, trading becomes more expensive and markets more fragile. Trading volume, depth and bid-ask spread responses also react mainly to *ERV* shocks. Figure 4 indicates that spreads increase for all asset classes within the first 5 minutes after an *ERV* shock. Thus, the slight decrease in bid-ask spread after an *IV* shock can be fully attributed to the responses after a *VRP* shock. In contrast, a textERV shock seems to impact liquidity providers such that liquidity deteriorates. Similarly, depth declines substantially for all asset classes after an *ERV* shock, strongly exceeding the liquidity adjustment in response to an *VRP* shock.

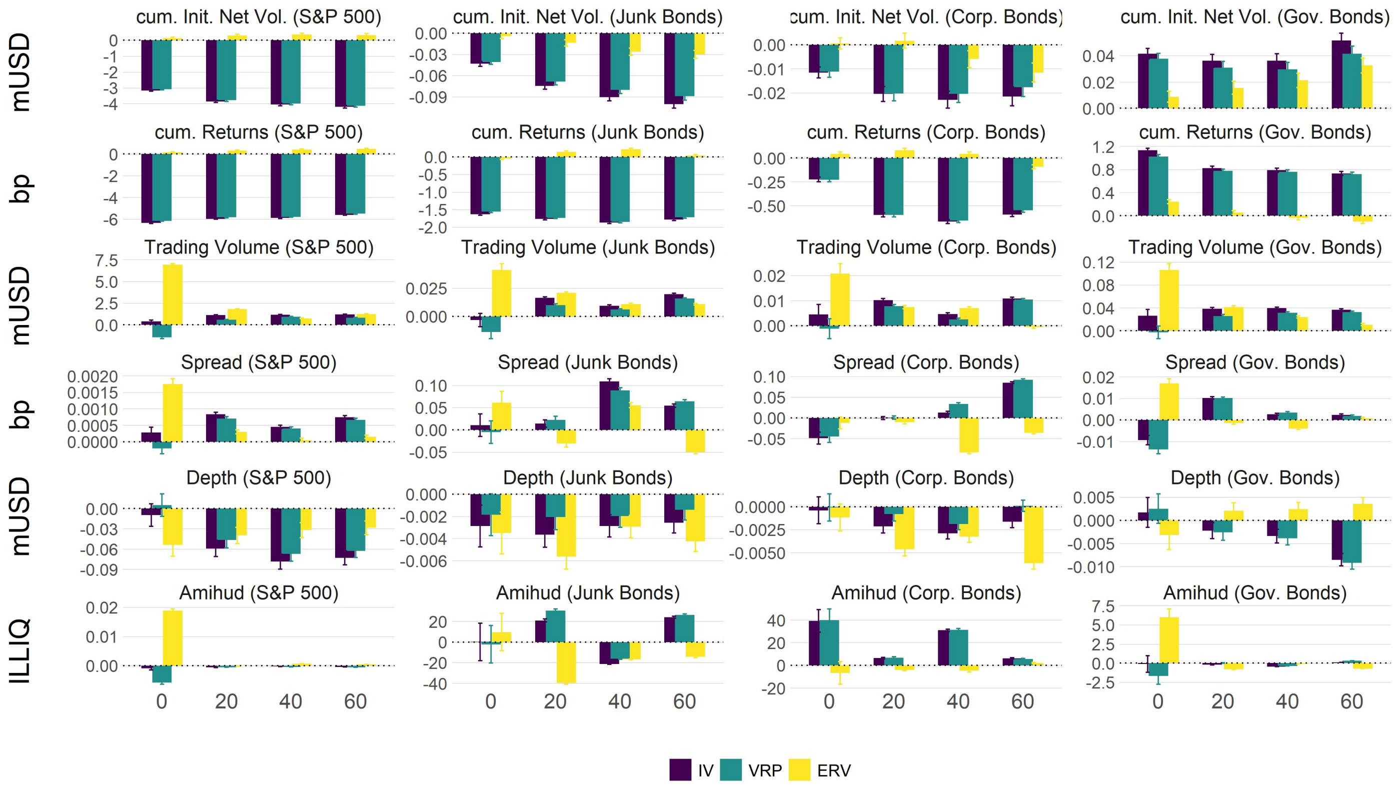

Figure 4: Estimated impulse response functions for the three different measures of risk, *IV* are the standardized implied variance changes, *ERV* is the standardized change in expected realized volatility and *VRP* is the standardized change in the variance risk premium, measured as $\widetilde{VRP}_{t,\tau} = IV_{t,\tau} - \widetilde{E}_{t,\tau}\left(RV^{(22)}_{t,\tau}\right)$. We always impose a positive shock of size one standard deviation. *Returns* and *initiator net volume* responses denote *cumulative* responses, whereas for *trading volume*, *depth*, *ILLIQ* and *bid-ask spread* we report impulse responses. We report *Return* and *bid-ask spread* responses in basis points, and denote the remaining variables in million USD. *Horizon* denotes the instantaneous (0 minute), 20 minute, 40 minute and 60 minute responses.

4.2.3 Crisis periods

Figure A2 in the Appendix provides a comparison of the (instantaneous) standardized response coefficients based on different sample periods: We impose a positive one standard deviation shock on *IV changes* during the Global Financial Crisis (*GFC*) (September 1st, 2008 until September 1st, 2009), *COVID-19* (February 15th, 2020 until February 15th, 2021) and the period in between (September 2nd, 2009 until February 14th, 2020). Similarly, we compute the responses to shocks in the *VRP* or the *ERV*, respectively. The ILLIQ measure decreases after an *ERV* shock. The response is particularly pronounced during the two crisis periods in our sample. We do find close to zero but negative instantaneous initiated net volume except for the Global Financial Crisis. This finding is in contrast to the surprising finding of *net buying* of the risky asset after an *ERV* shock. While such net selling is not an equilibrium result of our model we nevertheless attribute the large difference between the responses to a *VRP* and an *ERV* shock.

4.3 Institutional client response to a VIX shock

In order to shed light on the channels which drive the initiator net volume dynamics, we exploit institutional transaction data to compute explicitly responses in signed volume which is caused by orders of institutional clients. For that purpose, we retrieve all available client transactions from data provider Abel Noser for the period from January 2009 until April 2013 which trade one of the four ETFs in our sample. The Abel Noser sample is a proprietary dataset of institutional trading transactions and provides specific client trading execution which includes the side, execution price, the number of shares traded, intraday timestamps marking the order placement (when the institutional trader places the order with an external broker) and order execution.[8]

We retrieve the Abel Noser client transaction data and compute a measure for *client net volume* for each trading day and 5-minute interval for each of the tickers. We provide details for the construction of the measure in the Appendix. Client net volume measures the executed net initiated volume from institutional clients in million USD. We thus merge the order book and the client net volume data to estimate the responses of institutional client net volume to an *IV* shock as well as a shock in *VRP* and *ERV*. To that end, we re-estimate the coefficients of the impulse response function based on the entire available sample period (January 2009 until April 2013 for Abel Noser data) which include the 24 order book variables from Section 4 and

[8]For a detailed description of the Abel Noser dataset, consult Hu et al. (2018).

the 5-minute time series of initiated net volume.

In the same spirit as in Section 4, we impose a shock of one positive standard deviation in changes of either $IV_{t,\tau}$ or $ERV_{t,\tau}$ or $VRP_{t,\tau}$. Figure A3 in the Appendix illustrates the resulting response coefficients. The responses of client net volume largely mirror initiator net volume and thus reinforce our findings regarding the general dynamics. Specifically, we find that institutional trading responds to an *IV* shock with initiated selling of equity at large magnitudes as well. The flight to safety can be entirely attributed to a shock in *VRP*. Further, institutional client net volume turns *positive* after an *ERV* shock.

5 A model to disentangle the responses

Our empirical results provide evidence relating a VIX impulse to flight to safety and to market fragility, but these are due to separate channels. Increases in risk aversion as measured by a *VRP* impulse trigger active re-allocation from equities to government bonds, without market liquidity becoming impaired. Changes in cash-flow risk as measured by an *ERV* impulse, do *not* trigger a flight-to-safety, but do seem to impair market liquidity, at least contemporaneous. The surprising finding is that *active buying* of equities accompanies this market fragility.

Inspired by Grossman and Stiglitz (1980), Vayanos and Wang (2012) propose a simple, unified model to study how a variety of frictions affect asset returns and market liquidity. We extend their model along two dimensions: i) we include risk aversion shocks by letting some agents experience an increase in their coefficient of absolute risk aversion ("*VRP* channel"), and ii) we model a market with elevated cash-flow risks ("*ERV* channel"). We compare the extended set of equilibrium results to rationalize our findings on how risk aversion shocks or cash flow risk shocks affect prices due to initiator net volume and liquidity in form of price impact. We present the baseline model of Vayanos and Wang (2012) succinctly before introducing the model extensions.

5.1 Baseline model

The model features three periods indexed by $t \in \{0, 1, 2\}$. The market consists of a riskless and a risky asset. The riskless asset is in supply of B shares and pays one unit of consumption in Period 2. The risky asset is in supply of $\bar{\theta}$ shares and pays $D \sim N(\bar{D}, \sigma^2)$ units of consumption in Period 2. Using the riskless asset as numéraire, let S_t be the risky asset's price in Period t. By definition, $S_2 = D$.

There is a measure one of risk averse agents with exponential utility function, who derive utility from consumption C in Period 2:

$$U(C) = -\exp(-\alpha C), \tag{20}$$

where $\alpha > 0$ is the coefficient of absolute risk aversion. Agents are identical in Period 0 and endowed with identical supply of the assets.

We generate trade as follows: Just before Period 1, a fraction π of the agents learns that they will receive an endowment $z(D - \bar{D})$ of the consumption good in Period 2, with $z \sim N(0, \sigma_z^2)$, where z is independent of D. Since this endowment shock is perfectly correlated with D, the endowment creates hedging demand for the shocked agents in Period 1. For $z > 0$, for example, the agents can hedge this risk by selling the risky asset. These agents therefore initiate trades in Period 1 and are considered liquidity demanders. The remaining agents accommodate these trades and are considered liquidity suppliers.

5.2 Model extensions: Risk shocks

We add a *risk aversion shock* to the baseline model by letting the fraction π of agents that receive the endowment shock simultaneously experience an increase of their risk aversion to $\alpha' > \alpha$. Even absent of an endowment, the sudden risk aversion shock triggers re-allocations, which are absorbed by liquidity providers.

We model an increased *cash flow risk* for the (identical) agents in Period 0, where it is common knowledge that liquidity demanders learn additional information in Period 1 when observing a private signal:

$$s = D + \varepsilon, \tag{21}$$

where ε is normal with mean zero and variance σ_ε^2, and ε is independent of D and z. Note that we do not land in a no-trade theorem, since these agents also trade due to an endowment shock (Milgrom and Stokey, 1982). To consider the case of a Period 0 risk *cash flow risk increase* from the baseline model σ^2 to $\sigma^{2\prime\prime} > \sigma^2$, we set:

$$\sigma_\varepsilon^2 = \frac{\sigma^2 \sigma''^2}{\sigma''^2 - \sigma^2}, \tag{22}$$

Given the joint normality of (D, ε) the posterior risk for liquidity demanders after observing the signal s in Period 1 becomes:

$$\sigma^2(D|s) = \frac{\sigma_\varepsilon^2}{\sigma''^2 + \sigma_\varepsilon^2}\sigma''^2 = \sigma^2, \tag{23}$$

which is the baseline model cash flow risk. The liquidity demander who received the signal in Period 1 therefore experiences the same risk as the baseline model. The increased cash flow risk is experienced by the uninformed liquidity suppliers in Period 1, and, therefore, by all agents in Period 0 before they learn their type (i.e., liquidity demander or supplier). The uninformed experience the additional cash-flow risk for the simple reason that they are *uninformed*. They heard there is news. They understand others have access to the news. Ergo, in equilibrium, they prefer to reduce their risky asset holdings. The informed have observed the news and, therefore, bear less posterior risk. An alternative interpretation of the cash flow risk shock is that the more precise the signal (lower signal variance ε), the higher the relative information asymmetry between liquidity demanders and providers.

5.3 Equilibrium quantities and comparative statics

To investigate how equilibrium responses depend on risk aversion shocks and cash flow risk shocks, we focus on *initiator net volume,* which we define as the signed volume of liquidity demanders in Period 1 and the *price impact* of the liquidity demanders' trades in Period 1. We refer to price impact as λ, the coefficient of a regression of the price change between Periods 0 and 1 on the signed volume of liquidity demanders in Period 1. Intuitively, when λ is large, trades have large price impact, and we consider the market illiquid. Proposition 1 characterizes the relevant equilibrium quantities for the baseline model and the two distinct model extensions with *cash flow risk* and *risk aversion* shocks, respectively.

Proposition 1. ***(Equilibrium quantities)****. The equilibrium quantities for the baseline model, the model with a risk aversion shock, and the model with a cash flow risk shock are summarized below. The equilibrium quantities in the risk aversion-shock case are denoted by a prime, and the ones in the cash flow-risk case are denoted by a double prime. The initiator net volume* *results are:*

$$\nu = -\pi (1-\pi) z, \tag{24}$$

$$\nu' = \nu - \pi \left(1 - \frac{\bar{\alpha}}{\alpha'}\right)\left(\pi z + \bar{\theta}\right), \tag{25}$$

$$\nu'' = \pi \frac{(1-b)\,\sigma''^2 \bar{\theta}}{\sigma^2} + \pi \frac{(\beta_s - b)}{\alpha \sigma^2}\left(s - \bar{D}\right) - \pi \left(1 - \frac{bc}{\alpha\sigma^2}\right) z \tag{26}$$

where $\alpha' > \bar{\alpha} := \frac{1}{(1-\pi)\frac{1}{\alpha} + \pi \frac{1}{\alpha'}} > \alpha$ *and*

$$b = \frac{\pi\sigma^2 (D|S_1)\beta_s + (1-\pi)\,\sigma^2 \beta_\xi}{\pi\sigma^2 (D|S_1) + (1-\pi)\,\sigma^2} \tag{27}$$

$$c = \alpha\sigma_\varepsilon^2 \tag{28}$$

$$\beta_s = 1 - \frac{\sigma^2}{\sigma''^2}, \tag{29}$$

$$\beta_\xi = \frac{\sigma''^2}{\sigma''^2 + \sigma_\varepsilon^2 + c^2\sigma_z^2}, \tag{30}$$

$$\sigma^2 (D|S_1) = \beta_\xi \left(\sigma_\varepsilon^2 + c^2 \sigma_z^2\right). \tag{31}$$

The equilibrium price impacts are given by

$$\lambda = \frac{\alpha\sigma^2}{1-\pi}, \tag{32}$$

$$\lambda' = \frac{\bar{\alpha}\sigma^2}{1 - \pi + \pi\left(1 - \frac{\bar{\alpha}}{\alpha'}\right)} \tag{33}$$

$$\lambda'' = \frac{\alpha\sigma^2 (D|S_1)}{(1-\pi)\left(1 - \frac{\beta_\xi}{b}\right)}. \tag{34}$$

We provide all proofs in the Appendix.

We derive our main empirical predictions based on the equilibrium quantities in Proposition 1 for initiator net volume and the price impact measure. Note that the expected interim liquidity shock equals to $z = E(z) = 0$ and, for the cash flow risk model, the interim signal is $s = E(s) = \bar{D}$.

In expectation, trading decisions therefore do not reflect hedging needs due to endowment or information asymmetries, but only rely on either a change in the risk aversion for liquidity demanders or to a cash flow risk shock for liquidity providers.

Corollary 1. ***(Initiator net volume)***. *The expected equilibrium quantities for initiator net vol-*

ume, defined as the signed volume of liquidity demanders are such that

$$E(\nu') < E(\nu) = 0 < E(\nu'') \tag{35}$$

Note first, that the expected initiator net volume for the baseline model is zero, $E(\nu) = 0$. Intuitively, this reflects that only the endowment of liquidity demanders, which is centered around zero, generates trading. In contrast, Corollary 1 shows that initiator net volume $E(\nu')$ is negative in response to a risk aversion shock: Upon realizing a shock in their preferences, liquidity demanders re-allocate their portfolio and dispose of the risky asset. The re-allocation results in initiated net selling of the risky asset and net buying of the numéraire (safe asset). In other words: After a risk aversion shock, liquidity demanders are net sellers of the risky asset (and they pay an additional liquidity premium to incentivize liquidity providers for holding more units of the risky asset).

For the cash flow risk shock, receiving the signal triggers net initiated *buying* of the risky asset. Upon receiving the signal, liquidity demanders experience a reduced uncertainty with respect to future cash flow risks relative to liquidity providers. As a result, liquidity demanders re-allocate their portfolio by increasing their holdings of the risky asset. Liquidity providers learn that their uncertainty with respect to D did not get resolved and are willing to dispose of the asset.

Corollary 2. ***(Price impacts)****. The equilibrium quantities for price impact are such that*

$$0 < \lambda = \lambda' < \lambda'' \tag{36}$$

Price impact is positive for each model, such that return responses reflect the direction of initiated net volume. Corollary 2 illustrates for the risk aversion shock, that, irrespective of the choice of α', the price impact λ' remains the same as for the benchmark model, λ. Thus, risk aversion shocks do not imply that trades have larger price impact. For cash flow risk shocks, on the other side, initiator net volume moves prices more relative to the benchmark case without any information asymmetries. Thus, although liquidity providers learn about the signal from observed order flow, their information is less precise as that of the liquidity demanders. Therefore, liquidity providers require a higher compensation relative to the benchmark model.

To conclude, the theoretical framework provides the following main insights, in line with our empirical findings:

1. Risk aversion shocks trigger net selling of the risky asset and simultaneously net buying of government bonds as a response to re-allocations triggered by the shift in preferences.

Liquidity remains largely unaffected.

2. Cash flow shocks generate positive initiator net volume because they resemble a relative increase in risk for liquidity providers that did not receive a signal.

3. Price impact increases in response to cash flow risk shocks.

6 Conclusion

We set out to study the connection between flight-to-liquidity and market fragility. Our key contribution over a mature literature in both areas, is to analyze their joint *intraday* dynamics. We believe that any hope for unraveling their interrelationship requires a high-frequency analysis. Among the various approaches one could take, we picked one where a risk shock hits the market: A surprise increase in VIX or, shorter, a VIX impulse. Is there a flight to liquidity? Does market liquidity deteriorate?

The empirical analysis of 2007-2021 NASDAQ ETF trading yields some surprising results. While we find that a plain-vanilla VIX impulse leads to active re-allocation from equities to government bonds, there is no economically meaningful deterioration in liquidity. However, if we decompose VIX impulses into those driven by risk-aversion increases and those driven by cash-flow risk increases, then we *do* find a liquidity fragility result. The responses to risk-aversion increases largely resemble those of overall VIX impulses. The responses to cash-flow risk increases, however, are worse liquidity and *net* buying of equities (instead of net selling in the risk-aversion case). For a sub-period for which we have institutional flow data, we confirm this result of net buying after a cash-flow risk shock, but net selling after a risk-aversion shock.

We offer a way to understand our surprising finding by endowing a Grossman and Stiglitz (1980) trading model with the two types of risk shocks: A risk-aversion shock or a shock in cash-flow risk. Equilibrium trading replicates the unsurprising finding of flight-to-safety on a risk aversion shock, but also generates net-buying of risky assets and impaired liquidity on a cash-flow risk shock. The intuition for the latter result is that, in equilibrium, liquidity suppliers are least informed of news driving cash-flow risk shocks, therefore bear higher posterior risk, and thus prefer to hold relatively less of it. Liquidity demanders become the net buyers. The increased information asymmetry between suppliers and demanders of liquidity that drives this result is also the reason for worse liquidity. Liquidity suppliers experience larger adverse-selection costs and thus equilibrium liquidity supply deteriorates. In a way, this result tells us that if there is a cash-flow risk increase out there, then there are likely to be some who learn whether the news is good or bad for cash flows, and these are unlikely to be the liquidity suppliers.

Our findings add both evidence and an understanding to the debate on how markets respond to risk shocks and, relatedly, how to make them more resilient. We believe that more research on high-frequency dynamics is warranted: Do retail investors respond the same way to the two types of shocks as institutional investors? How do market makers respond? Do our findings hold internationally? The current trend of mandatory disclosure of transactions to trade repositories makes more data available. This "big data" build-up along with rapid development in machine-learning techniques to unravel potential non-linearity, enables further study to deepen our understanding of how markets respond to risk shocks. Such understanding we deem to be of first-order importance, not only to academics, but also to industry participants and regulators.

References

Adrian, T., R. K. Crump, and E. Vogt (2019). Nonlinearity and Flight-to-Safety in the Risk-Return Trade-Off for Stocks and Bonds. *The Journal of Finance 74*(4), 1931–1973.

Ait-Sahalia, Y., F. Matthys, E. Osambela, and R. Sircar (2021). When Uncertainty and Volatility Are Disconnected: Implications for Asset Pricing and Portfolio Performance. Working paper.

Amihud, Y. (2002). Illiquidity and Stock Returns: Cross-section and time-series Effects. *Journal of Financial Markets 5*(1), 31–56.

Angel, J. J., L. E. Harris, and C. S. Spatt (2015). Equity Trading in the 21st Century: An Update. *Quarterly Journal of Finance 5*.

Baele, L., G. Bekaert, K. Inghelbrecht, and M. Wei (2019). Flights to Safety. *Review of Financial Studies 33*(2), 689–746.

Beber, A., M. W. Brandt, and K. A. Kavajecz (2009). Flight-to-Quality or Flight-to-Liquidity? Evidence from the Euro-Area Bond Market. *Review of Financial Studies 22*, 925–957.

Bekaert, G. and M. Hoerova (2014). The VIX, the Variance Premium and Stock Market Volatility. *Journal of Econometrics 183*, 181–192.

Bekaert, G., M. Hoerova, and M. L. Duca (2013). Risk, Uncertainty and Monetary Policy. *Journal of Monetary Policy 60*, 771–788.

Bekaert, G., M. Hoerova, and N. R. Xu (2021). Risk, Monetary Policy and Asset Prices in a Global World. Working paper.

BIS and IOSCO (2012). Principles for Financial Market Infrastructures. Manuscript, Committee on Payment and Settlement Systems and Technical Committee of the International Organization of Securities Commissions.

Bollerslev, T., M. Gibson, and H. Zhou (2011). Dynamic Estimation of Volatility Risk Premia and Investor Risk Aversion from Option-implied and Realized Volatilities. *Journal of Econometrics 160*, 235–245.

Bollerslev, T., J. Marrone, L. Xu, and H. Zhou (2014). Stock Return Predictability and Variance Risk Premia: Statistical Inference and International Evidence. *Journal of Financial and Quantitative Analysis 49*, 633–661.

Bollerslev, T., N. Sizova, and G. Tauchen (2012). Volatility in Equilibrium: Asymmetries and Dynamic Dependencies. *Review of Finance 16*, 31–80.

Bollerslev, T., G. Tauchen, and H. Zhou (2009). Expected Stock Returns and Variance Risk Premia. *Review of Financial Studies 22*, 4463–4492.

Bollerslev, T., V. Todorov, and L. Xu (2015). Tail Risk Premia and Return Predictability. *Journal of Financial Economics 118*, 113–134.

Brenner, M. and Y. Izhakian (2018). Asset Pricing and Ambiguity: Empirical Evidence. *Journal of Financial Economics 130*(3), 503–531.

Brunnermeier, M. K. (2009). Deciphering the Liquidity and Credit Crunch 2007-2008. *Journal of Economic Perspectives 23*(1), 77–100.

Campbell, J. Y. and J. H. Cochrane (1999). By Force of Habit: A Consumption-Based Explanation of Aggregate Stock Market Behavior. *Journal of Political Economy 107*(2), 205–251.

Capponi, A., A. J. Menkveld, and H. Zhang (2021). Large Orders in Small Markets: The Value of Order Flow Predictability. Working paper.

Carr, P. (2017). Why is VIX a Fear Gauge? *Risk and Decision Analysis 6*, 179–185.

Carr, P. and L. Wu (2009). Variance Risk Premiums. *Review of Financial Studies 22*, 1311–1341.

Corsi, F. (2009). A Simple Approximate Long-Memory Model of Realized Volatility. *Journal of Financial Econometrics 7*(2), 174–196.

Drechsler, I. (2013). Uncertainty, Time-Varying Fear, and Asset Prices. *The Journal of Finance 68*(5), 1843–1889.

ESMA (2019). Guidelines on liquidity stress testing in UCITS and AIFs. Manuscript, European Securities and Markets Authority.

Grossman, S. J. and J. E. Stiglitz (1980). On the Impossibility of Informationally Efficient Markets. *American Economic Review 70*, 393–408.

Hendershott, T. and A. J. Menkveld (2014). Price Pressures. *Journal of Financial Economics 114*(3), 405–423.

Hu, G., K. M. Jo, Y. A. Wang, and J. Xie (2018). Institutional Trading and Abel Noser Data. *Journal of Corporate Finance 52*, 143–167.

Jorda, O. (2005). Estimation and Inference of Impulse Responses by Local Projections. *American Economic Review 95*(1), 161–182.

Koop, G., M. Pesaran, and S. M. Potter (1996). Impulse Response Analysis in Nonlinear Multivariate Models. *Journal of Econometrics 74*(1), 119 – 147.

Liu, J., J. Pan, and T. Wang (2004). An Equilibrium Model of Rare-Event Premia and Its Implication for Option Smirks. *The Review of Financial Studies 18*(1), 131–164.

Longstaff, F. A. (2004). The Flight-to-Liquidity Premium in U.S. Treasury Bond Prices. *Journal of Business 77*, 511–526.

Milgrom, P. and N. Stokey (1982). Information, Trade and Common Knowledge. *Journal of Economic Theory 26*, 17–27.

Montiel Olea, J. L. and M. Plagborg-Møller (2021). Local Projection Inference Is Simpler and More Robust Than You Think. *Econometrica 89*(4), 1789–1823.

Pedersen, L. H. (2009). When Everyone Runs for the Exit. *International Journal of Central Banking 5*, 177–199.

Pesaran, H. and Y. Shin (1998). Generalized Impulse Response Analysis in Linear Multivariate Models. *Economics Letters 58*(1), 17 – 29.

Rosenberg, J. and R. F. Engle (2002). Empirical Pricing Kernels. *Journal of Financial Economics 64*, 341–372.

SEC (2016). Investment Company Liquidity Risk Management Programs. Manuscript, SEC Release No. 33–10233.

Sims, C. (1980). Macroeconomics and Reality. *Econometrica 48*, 1 – 48.

Vayanos, D. and J. Wang (2012). Liquidity and Asset Returns Under Asymmetric Information and Imperfect Competition. *Review of Financial Studies 25*, 1339–1365.

		2007	2008	2009	2010	2011	2012	2013	2014	2015	2016	2017	2018	2019	2020	2021	Total
S&P 500	Amihud Measure	0.07 (0.06)	0.08 (0.08)	0.12 (0.09)	0.11 (0.09)	0.12 (0.1)	0.11 (0.09)	0.12 (0.09)	0.13 (0.11)	0.17 (0.15)	0.21 (0.18)	0.16 (0.15)	0.17 (0.15)	0.15 (0.12)	0.2 (0.16)	0.14 (0.12)	0.14 (0.13)
	Transaction size	2.14 (0.23)	1.48 (0.51)	1.06 (0.21)	1.12 (0.18)	0.98 (0.2)	1.24 (0.17)	1.2 (0.15)	1.14 (0.17)	0.98 (0.18)	0.92 (0.17)	1.17 (0.13)	0.82 (0.18)	0.77 (0.13)	0.65 (0.15)	0.76 (0.12)	1.08 (0.36)
	Depth (Best Level)	3.46 (1.58)	2.33 (1.14)	2.13 (0.71)	2.85 (1.14)	1.93 (0.95)	2.69 (1.06)	2.49 (0.95)	2.41 (1.11)	1.29 (0.87)	0.85 (0.32)	1.1 (0.42)	0.61 (0.33)	0.63 (0.37)	0.35 (0.19)	0.45 (0.2)	1.71 (1.24)
	Depth (50bp)	330.36 (126.27)	204.75 (91.82)	149.01 (51.53)	236.59 (78.91)	125.04 (55.99)	96.82 (32.87)	112.52 (52.48)	126.72 (51.05)	50.97 (14.95)	35.58 (7.05)	41.23 (7.06)	31.02 (7.8)	35.94 (9.39)	21.91 (5.09)	21.23 (3.62)	104.9 (94.03)
	Depth (5bp)	140.96 (55.09)	84.27 (46.25)	41.22 (11.07)	69.15 (15.3)	49.97 (17.61)	50.89 (13.71)	70.41 (30.83)	87.99 (33.31)	31.45 (10.3)	19.96 (5.04)	28.34 (4.93)	20.39 (6.49)	22.26 (6)	13.33 (4.95)	15.45 (3.41)	48.38 (37.54)
	Depth imbalance	-0.05 (8.85)	-0.28 (4.64)	-0.15 (2.91)	0.01 (3.91)	0.25 (2.72)	0.07 (1.96)	0.29 (3.39)	0.01 (3.67)	-0.27 (3.52)	-0.01 (1.36)	-0.17 (2.02)	0.07 (1.44)	0.02 (1.86)	-0.08 (1.22)	0.06 (1.15)	-0.02 (3.27)
	Return	-0.05 (10.53)	-0.08 (20.97)	0.08 (13.66)	0.03 (9.15)	-0.02 (10.75)	0.06 (6.33)	0.08 (5.58)	0 (6.01)	0.03 (7.41)	0.06 (6.91)	0.05 (3.67)	-0.09 (9.31)	0.08 (6.23)	0.01 (15.26)	0.07 (8.68)	0.02 (10.38)
	Initiator net volume	0.46 (30.94)	2.46 (30.74)	-0.65 (16.04)	-0.08 (13.17)	-0.49 (14.4)	-0.04 (9.2)	-0.16 (7.26)	0.1 (7.19)	0.35 (9.1)	-0.17 (5.53)	0.12 (5.15)	-0.2 (8.14)	0.06 (7.67)	0.21 (8.85)	-0.2 (6.99)	0.12 (13.8)
	Bid-ask Spread	0.8 (0.09)	1 (0.25)	1.16 (0.19)	0.91 (0.06)	0.85 (0.1)	0.76 (0.04)	0.65 (0.04)	0.58 (0.04)	0.57 (0.05)	0.56 (0.06)	0.46 (0.04)	0.48 (0.15)	0.41 (0.05)	0.5 (0.16)	0.34 (0.06)	0.68 (0.25)
	Trade ratio	0.01 (0)	0.01 (0)	0.02 (0)	0.01 (0)	0.01 (0.01)	0.01 (0)	0.01 (0)	0.01 (0)	0.01 (0)	0.01 (0)	0.01 (0)	0.02 (0.01)	0.01 (0)	0.01 (0.01)	0.01 (0)	0.01 (0.01)
	Trading volume	130.05 (106.14)	172.77 (120.91)	88.22 (61.11)	68.71 (58.93)	68.25 (54.79)	47.71 (34.94)	38.34 (32.25)	35.96 (30.56)	34.87 (29.7)	24.57 (20.76)	18.89 (15.67)	39.97 (35.54)	32 (27.73)	46.91 (44.62)	48.77 (39.33)	57.83 (67.15)
Junk Bonds	Amihud Measure	2305.56 (14446.31)	1370.56 (12876.92)	630.8 (10737.48)	156.89 (2238.3)	130.25 (1498.62)	25.18 (154.42)	17.37 (185.35)	15.63 (217.82)	9.44 (228.44)	6.44 (125.83)	3.35 (26.45)	2.57 (25.28)	2.22 (56.26)	1.95 (4.09)	2.13 (24.08)	136.17 (4037.61)
	Transaction size	0.21 (0.17)	0.31 (0.2)	0.17 (0.05)	0.18 (0.05)	0.2 (0.05)	0.24 (0.06)	0.29 (0.06)	0.36 (0.09)	0.39 (0.09)	0.41 (0.08)	0.53 (0.12)	0.62 (0.12)	0.85 (0.2)	0.51 (0.24)	0.55 (0.09)	0.38 (0.23)
	Depth (Best Level)	0.1 (0.13)	0.29 (0.37)	0.08 (0.11)	0.08 (0.12)	0.11 (0.1)	0.13 (0.1)	0.19 (0.12)	0.25 (0.16)	0.3 (0.18)	0.36 (0.14)	0.6 (0.25)	0.82 (0.39)	2.39 (1.1)	1.35 (1.08)	1.2 (0.81)	0.53 (0.78)
	Depth (50bp)	0.22 (0.2)	1.87 (1.32)	0.61 (0.51)	1.29 (0.86)	2.01 (1.39)	2.61 (0.98)	3.43 (0.88)	3.15 (1.14)	3.37 (1.39)	3.35 (0.62)	5.79 (1.3)	11.44 (4.44)	24.85 (7.76)	14.51 (6.17)	13.1 (5.29)	5.9 (7.36)
	Depth (5bp)	0.11 (0.14)	0.43 (0.47)	0.14 (0.16)	0.26 (0.34)	0.43 (0.37)	0.61 (0.31)	0.99 (0.41)	1.3 (0.51)	1.43 (0.58)	1.54 (0.39)	2.52 (0.64)	3.57 (1.19)	9.6 (3.46)	4.76 (3.08)	4.25 (2.34)	2.08 (2.85)
	Depth imbalance	-0.02 (0.14)	-0.25 (0.45)	-0.05 (0.16)	-0.03 (0.3)	-0.1 (0.34)	-0.02 (0.26)	-0.01 (0.38)	0.03 (0.45)	0.01 (0.38)	0.01 (0.31)	0.06 (0.56)	0.03 (0.82)	0.33 (1.95)	0.11 (1.12)	0.27 (1.11)	0.01 (0.74)
	Return	-0.1 (11.37)	0.01 (15.08)	0.07 (13.27)	0.03 (6.43)	0.05 (6.08)	0.02 (3.27)	0 (3.04)	-0.02 (2.73)	0.01 (3.24)	0.09 (3.82)	0.01 (1.81)	-0.01 (2.59)	0.05 (2.08)	0.01 (7.38)	0 (2.51)	0.02 (6.99)
	Initiator net volume	0 (0.03)	0.02 (0.16)	0.01 (0.16)	0 (0.2)	0 (0.23)	0.01 (0.26)	-0.01 (0.35)	-0.01 (0.39)	0 (0.6)	0 (0.66)	0.01 (0.65)	0 (0.85)	0.02 (1.43)	0.02 (1.53)	-0.02 (1.26)	0 (0.72)
	Bid-ask Spread	77.83 (48.23)	32.12 (35.01)	16.63 (16.49)	5.41 (4.99)	4.73 (3.81)	2 (1.28)	1.37 (0.47)	1.24 (0.3)	1.25 (0.32)	1.26 (0.14)	1.16 (0.06)	1.18 (0.04)	1.17 (0.03)	1.29 (0.38)	1.18 (0.05)	8.01 (21.26)
	Trade ratio	0.08 (0.22)	0.11 (0.23)	0.04 (0.05)	0.02 (0.02)	0.03 (0.03)	0.02 (0.02)	0.02 (0.02)	0.02 (0.02)	0.02 (0.01)	0.01 (0.01)	0.02 (0.01)	0.01 (0.01)	0.01 (0.01)	0.01 (0.01)	0.01 (0.01)	0.03 (0.07)
	Trading volume	0 (0.03)	0.04 (0.15)	0.1 (0.18)	0.1 (0.25)	0.15 (0.3)	0.3 (0.39)	0.37 (0.57)	0.43 (0.7)	0.8 (1.18)	1.15 (1.31)	0.89 (1.26)	1.25 (1.67)	1.84 (2.44)	2.95 (2.96)	2.16 (2.38)	0.79 (1.57)
Corporate Bonds	Amihud Measure	843.5 (4746.57)	960 (9204.07)	142.37 (1266.37)	107.53 (785.24)	113.88 (1066.7)	43.54 (426.51)	64.56 (574.19)	77.79 (687.11)	68.08 (2132.8)	22.36 (327.71)	10.68 (139.55)	11.16 (241.98)	4.63 (114.2)	2.24 (5.42)	2.02 (3.21)	124.75 (2533.65)
	Transaction size	0.26 (0.14)	0.3 (0.16)	0.26 (0.08)	0.25 (0.09)	0.33 (0.13)	0.33 (0.1)	0.28 (0.08)	0.26 (0.08)	0.28 (0.07)	0.33 (0.07)	0.45 (0.11)	0.54 (0.13)	0.52 (0.1)	0.44 (0.13)	0.42 (0.06)	0.35 (0.14)
	Depth (Best Level)	0.31 (0.34)	0.23 (0.27)	0.14 (0.2)	0.1 (0.14)	0.18 (0.36)	0.22 (0.36)	0.13 (0.25)	0.1 (0.11)	0.1 (0.09)	0.18 (0.11)	0.42 (0.17)	0.47 (0.17)	0.54 (0.2)	0.41 (0.25)	0.61 (0.2)	0.26 (0.27)
	Depth (50bp)	2.21 (0.87)	1.75 (1.06)	2.27 (1.4)	2.96 (1.88)	3.37 (2)	3.25 (1.89)	4.47 (3.1)	1.14 (0.5)	1.47 (0.7)	2.28 (0.93)	7.48 (2.01)	6.89 (2.23)	8.85 (2.28)	9.55 (4.87)	13.7 (6.19)	4.36 (3.78)
	Depth (5bp)	0.69 (0.53)	0.51 (0.44)	0.33 (0.37)	0.56 (0.52)	0.75 (0.8)	0.97 (0.82)	0.62 (0.43)	0.42 (0.26)	0.51 (0.34)	1.02 (0.42)	3 (1.04)	2.61 (0.81)	3.57 (0.99)	2.08 (1.36)	3.03 (0.72)	1.31 (1.29)
	Depth imbalance	-0.38 (0.58)	-0.26 (0.47)	-0.13 (0.37)	-0.02 (0.47)	-0.13 (0.85)	-0.11 (0.8)	0.04 (0.41)	0 (0.19)	0 (0.14)	-0.01 (0.25)	-0.07 (0.85)	0 (0.51)	0.04 (0.61)	-0.04 (0.52)	-0.05 (0.58)	-0.06 (0.55)
	Return	-0.01 (5.25)	-0.09 (13.77)	0.06 (7.82)	0.01 (3.51)	0.06 (3.91)	0 (2.62)	-0.01 (2.98)	0.02 (2.5)	0.01 (3.11)	0.03 (2.72)	0.04 (1.93)	-0.03 (1.99)	0.03 (2.27)	-0.01 (6.98)	0.06 (3.13)	0.01 (5.37)
	Initiator net volume	0.01 (0.09)	0.04 (0.31)	0.01 (0.29)	-0.01 (0.23)	0.01 (0.52)	0.01 (0.44)	-0.02 (0.4)	-0.01 (0.22)	0 (0.31)	0.01 (0.32)	-0.01 (0.48)	0 (0.62)	0 (0.66)	0.02 (0.88)	0.05 (0.92)	0 (0.48)
	Bid-ask Spread	18.45 (11.67)	20.24 (19.25)	9.47 (9.7)	3.21 (3.07)	3.81 (2.62)	2.23 (1.25)	2.66 (1.81)	2.26 (1.47)	1.66 (1.28)	1.03 (0.86)	0.86 (0.1)	0.9 (0.13)	0.85 (0.07)	1.07 (1.24)	0.79 (0.07)	4.35 (8.63)
	Trade ratio	0.02 (0.06)	0.02 (0.04)	0.02 (0.03)	0.02 (0.02)	0.01 (0.01)	0.02 (0.02)	0.02 (0.03)	0.02 (0.02)	0.02 (0.01)	0.01 (0.01)	0.01 (0.01)	0.01 (0.01)	0.01 (0.01)	0.02 (0.01)	0.01 (0.01)	0.02 (0.02)
	Trading volume	0.03 (0.09)	0.11 (0.35)	0.18 (0.38)	0.14 (0.33)	0.25 (0.65)	0.27 (0.56)	0.25 (0.55)	0.16 (0.31)	0.27 (0.47)	0.44 (0.65)	0.55 (0.85)	0.82 (1.16)	1.13 (1.53)	1.99 (1.92)	1.74 (1.73)	0.51 (1.04)
Government Bonds	Amihud Measure	50.09 (547.08)	61.48 (1521.52)	20.87 (152.52)	7.31 (32.68)	2.74 (5.1)	7.02 (346.01)	4.32 (7.85)	3.83 (5.45)	3.36 (4.37)	4.36 (6.77)	2.65 (3.31)	2.5 (3.22)	2.13 (2.41)	1.82 (1.92)	1.53 (1.59)	10.86 (435.1)
	Transaction size	0.48 (0.14)	0.39 (0.12)	0.25 (0.04)	0.29 (0.04)	0.32 (0.04)	0.35 (0.06)	0.43 (0.06)	0.36 (0.05)	0.29 (0.04)	0.34 (0.07)	0.43 (0.07)	0.51 (0.07)	0.44 (0.09)	0.35 (0.05)	0.38 (0.05)	0.37 (0.1)
	Depth (Best Level)	0.37 (0.3)	0.31 (0.3)	0.23 (0.14)	0.61 (0.3)	0.55 (0.33)	0.24 (0.1)	0.38 (0.15)	0.36 (0.13)	0.29 (0.13)	0.26 (0.1)	0.37 (0.26)	0.44 (0.22)	0.45 (0.23)	0.25 (0.57)	0.4 (0.2)	0.37 (0.28)
	Depth (50bp)	6.13 (1.75)	10.5 (6.22)	7.83 (2.78)	19.88 (11.66)	17.59 (10)	6.63 (2.52)	12.85 (4.5)	12.84 (3.2)	11.99 (2.56)	12.15 (4.28)	16.23 (5.83)	16.72 (6.04)	12.26 (4.7)	8.27 (3.03)	14.66 (3.66)	12.55 (6.95)
	Depth (5bp)	2.87 (1.12)	2.4 (1.56)	2.13 (1.06)	9.85 (5.45)	9.73 (5.65)	3.18 (1.09)	6.89 (2.1)	7.09 (1.67)	6.31 (1.49)	5.37 (1.5)	6.46 (1.51)	6.53 (1.43)	5.74 (2.19)	3.79 (1.75)	6.47 (1.57)	5.72 (3.5)
	Depth imbalance	0.03 (1.55)	0.04 (1.62)	0.07 (0.54)	0.15 (1.05)	0.03 (0.54)	0.02 (0.59)	0.08 (1)	-0.07 (0.98)	-0.04 (0.55)	0.02 (0.56)	0.04 (1.09)	0.05 (1.01)	-0.02 (0.47)	0.01 (0.8)	0.01 (0.54)	0.03 (0.92)
	Return	0.08 (5.53)	-0.03 (8.98)	-0.04 (10.13)	-0.01 (7.57)	0.18 (8.93)	-0.05 (6.67)	-0.07 (6.05)	0.05 (5.26)	-0.04 (6.81)	0 (6.14)	0.07 (4.66)	-0.02 (4.73)	0.01 (5.24)	-0.06 (10.45)	0.06 (6.89)	0.01 (7.24)
	Initiator net volume	0.02 (0.61)	0 (0.79)	-0.02 (0.57)	-0.01 (0.73)	0 (0.97)	0.01 (0.67)	0.01 (0.76)	0.01 (0.6)	0.03 (0.72)	0.02 (0.69)	0.01 (1.05)	-0.01 (1.05)	0 (0.86)	0.01 (1.27)	0.06 (1.5)	0.01 (0.85)
	Bid-ask Spread	1.82 (0.54)	3.48 (2.98)	2.21 (1.04)	1.19 (0.33)	1.34 (0.59)	1.35 (0.38)	1.28 (0.54)	0.98 (0.2)	0.97 (0.27)	0.97 (0.14)	0.9 (0.09)	0.9 (0.07)	0.87 (0.09)	1.02 (0.93)	0.78 (0.09)	1.35 (1.17)
	Trade ratio	0.01 (0.01)	0.01 (0.01)	0.01 (0)	0 (0)	0.01 (0)	0.01 (0)	0.01 (0)	0.01 (0)	0.01 (0)	0.01 (0)	0.01 (0)	0.01 (0)	0.01 (0.01)	0.01 (0.01)	0.01 (0)	0.01 (0.01)
	Trading volume	0.5 (0.98)	0.77 (1.24)	0.92 (1.31)	1.95 (2.89)	3.84 (4.94)	2.56 (3.39)	1.83 (2.17)	1.63 (1.93)	2.25 (1.96)	1.62 (1.68)	2.06 (2.35)	2.29 (2.78)	2.69 (3.19)	4.09 (5.15)	4.45 (4.91)	2.17 (3.1)
	VIX change	-0.13 (62.21)	-0.53 (54.16)	-0.6 (37.98)	-0.64 (49.41)	0.25 (53.79)	-0.16 (47.27)	-0.24 (40.13)	0.17 (61.83)	-0.55 (69.47)	-0.73 (58.48)	-0.42 (61.89)	0.37 (91.15)	-1.44 (63.77)	-0.33 (78.28)	-0.99 (86.35)	-0.38 (61.27)

Table AI: Sample summary statistics. The values denote the sample means, values in brackets are the corresponding standard deviations. *Transaction size* is the average transaction size during each 5-minute window for each ticker in 100 thousand USD. We compute transaction sizes as the number of shares multiplied by the share price. Market orders that affect multiple levels of the order book are reported as individual messages with identical timestamp by NASDAQ, but are aggregated before computing the transaction sizes. *Depth* denotes the aggregate available number of shares within the best level, 5 or 50 basis points from the current best price (in million USD). *Depth Imbalance* is the net of buy limit orders and sell limit orders in the order book, 50 basis points around the best price of each side (in million USD) *Return* denotes the 5-minute log returns in basis points. *Initiator net volume* corresponds to the average aggregate initiator net volume during each 5-minute interval in million USD. We compute the aggregate number of shares multiplied by one if the transaction corresponds to an execution above the current midquote and minus one if the transaction executes at a price lower than the current midquote. *bid-ask spread* is the time-weighted average bid-ask spread in basis points. *Trade ratio* is the ratio of trade executions relative to the number of all messages. *Trading volume* is the executed transaction volume during each 5-minute window (in million USD). *Amihud (ILLIQ) measure* is computed by dividing the absolute value of 5 minute log returns (in basis points) by trading volume (in million USD). To make the values comparable, we always multiply the aggregate number of traded shares with the rolling 12-month average midquote computed for each ticker. The tickers denote the major ETFs tracking corporate bonds (*LQD*), S&P 500 (*SPY*), Junk Bonds (*HYG*) and government bonds (*TLT*). *VIX change* denotes the 5-minute log change of the VIX (CBOE Volatility Index) in basis points.

	#Orders	Volume (mean)	Volume (median)	Volume (95%)	Duration (mean)	Duration (25%)	Duration (median)	Duration (75%)	Duration (95%)
Junk Bonds	8816	0.213	0.010	0.237	13.816	5	5	5	35
Corporate Bonds	9569	0.176	0.016	0.311	27.507	5	5	5	205
S&P 500	75619	1.235	0.034	5.485	11.518	5	5	5	25
Government Bonds	3708	0.647	0.012	2.409	48.863	5	5	30	275

Table AII: Summary statistics for the Abel Noser transaction message data. We restrict the sample to transactions with reported placement and last trade timestamps within regular NASDAQ trading hours. *# Orders* is the total number of transactions within the sample. *Volume* is the total transaction size in million USD (computed as total traded shares multiplied with average transaction price per share). *Duration* is in minutes and denotes the reported duration of the transaction from placement date until last trade date.

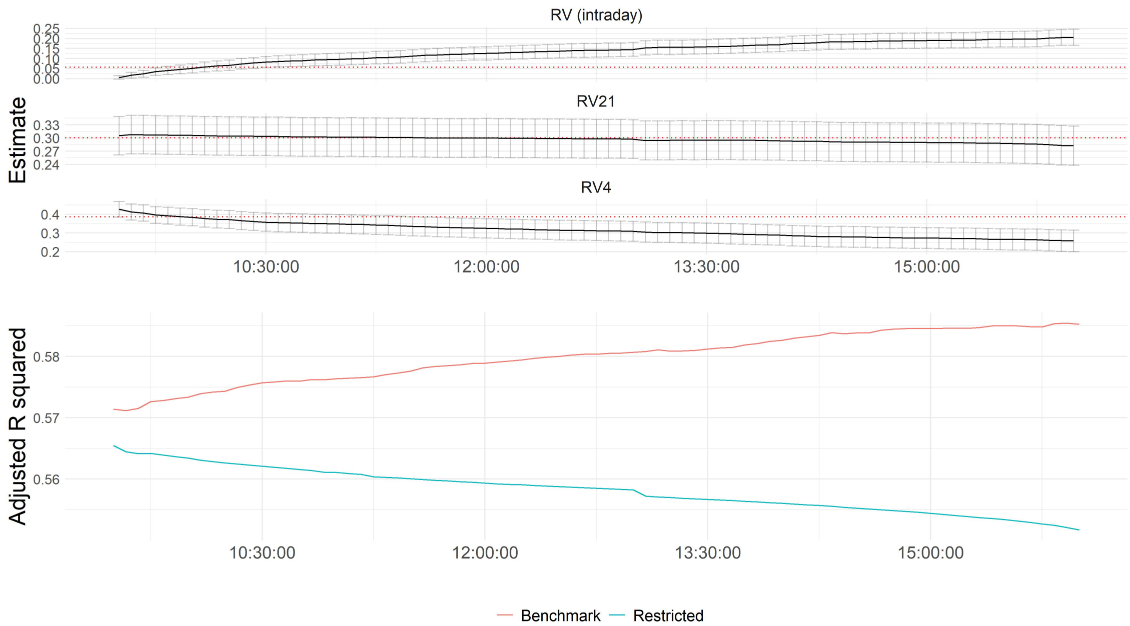

Figure A1: Panel 1 shows the estimated regression coefficient of the predictive regression $\log\left(RV^{(22)}_{t,\tau}\right) = c_\tau + \beta_\tau \log\left(RV^{(21)}_{t-22,0} + \widetilde{RV}_{t,\tau}\right) + \gamma_\tau \log\left(RV^{(4)}_{t-5,0} + \widetilde{RV}_{t,\tau}\right) + \delta_\tau \log\left(\widetilde{RV}_{t,\tau}\right) + \varepsilon_{t,\tau}$. The x-axis denotes the 5-minute intervals during the day, and the error bars correspond to 95% confidence intervals. The red dotted line indicates the regression coefficients when assuming that c, β, γ and δ are constant across timestamp τ. The second panel illustrates the adjusted R^2 of two different predictive regression models for the future realized variance. *Benchmark* corresponds to our main specification that predicts future realized variance. The *restricted* model omits $\widetilde{RV}_{t,\tau}$ in the regression and thus only incorporates information from past trading days.

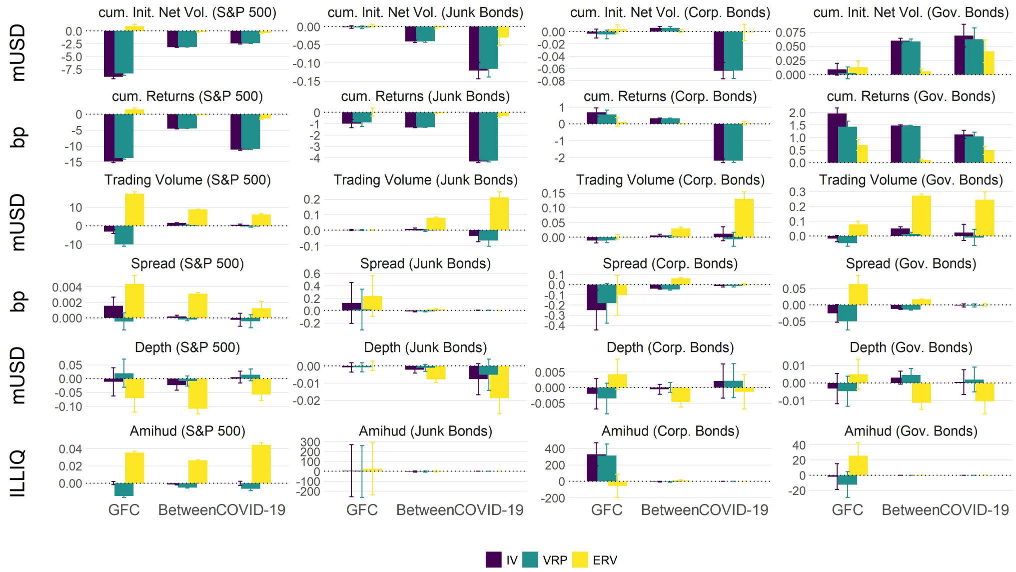

Figure A2: Estimated impulse response functions for the three different measures of risk, *IV* are the standardized implied variance changes, *ERV* is the standardized change in expected realized volatility and *VRP* is the standardized change in the variance risk premium, measured as $\widetilde{VRP}_{t,\tau} = IV_{t,\tau} - \widetilde{E}_{t,\tau}\left(RV^{(22)}_{t,\tau}\right)$. We always impose a positive shock of size one standard deviation. *Returns* and *initiator net volume* responses denote *cumulative* responses, whereas for *trading volume*, *depth* and *bid-ask spread* we report impulse responses. We report *Return bid-ask spread* and *ILLIQ* responses in basis points, and denote the remaining variables in million USD. We only report instantaneous responses. The sample periods correspond to the Global Financial Crisis (*GFC*) (September 1st, 2008 until September 1st, 2009), *COVID-19* (February 15th, 2020 until February 15th, 2021) and the period in between (September 2nd, 2009 until February 14th, 2020).

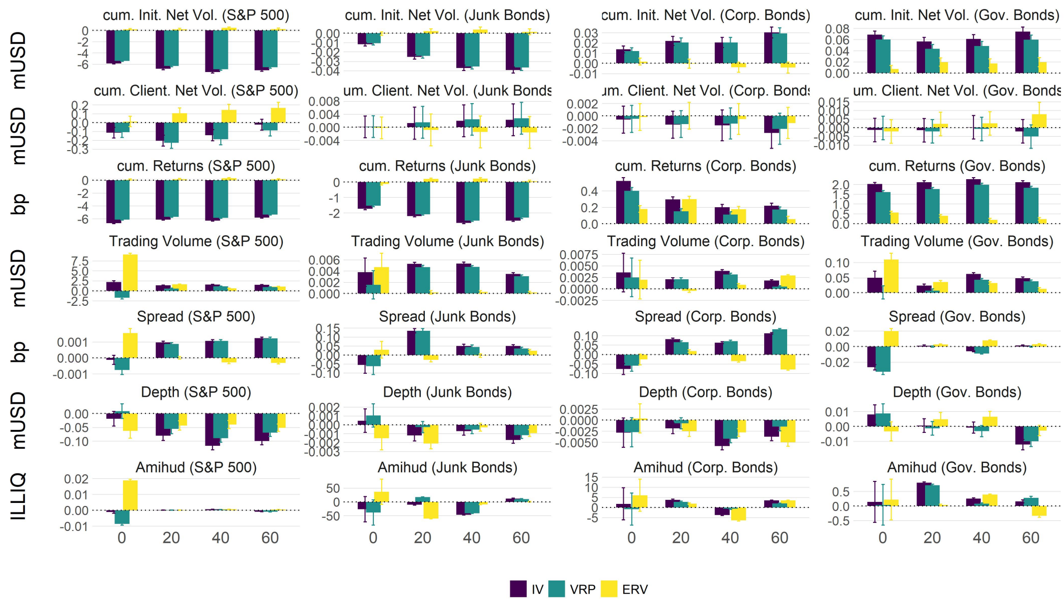

Figure A3: Estimated impulse response functions based on the entire sample period where Abel Noser data is available. We shock changes in $IV_{t,\tau}$, $ERV_{t,\tau}$ and $VRP_{t,\tau}$ by one standard deviation. *Initiator net volume*, *client net volume* and *Return* responses denote cumulative values, *trading volume, depth, bid-ask spread* and *ILLIQ* are the standard impulse responses. We report *Return* and *bid-ask spread* responses in basis points and denote all remaining variables in million USD. *Horizon* denotes the instantaneous (0 minute), 20 minute, 40 minute and 60 minute responses. The error bars illustrate 95% confidence intervals.

I Proofs and Lemmas

Proof. (Equations (17) and (18)) Under the assumption that $\hat{\boldsymbol{\beta}}_i^a(h)$ and $\hat{\boldsymbol{\Sigma}}_{\boldsymbol{u}}$ are asymptotically independent, Equation (17) follows directly from Appendix A in Pesaran and Shin (1998). In fact, Equation (17) is a special case of (A.15) in Pesaran and Shin (1998) if only estimates of $\boldsymbol{\beta}_i^a(h) = \boldsymbol{\Phi}_h' \boldsymbol{e}_i$ (estimated through local projections) and their asymptotic covariances $AV[\hat{\boldsymbol{\beta}}_i^a(h)]$ are available. The asymptotic independence of $\hat{\boldsymbol{\beta}}_i^a(h)$ and $\hat{\boldsymbol{\Sigma}}_{\boldsymbol{u}}$ is implied by the assumption of multivariate normality of the VAR errors $\boldsymbol{u}_\tau$ and the interpretation of $\hat{\boldsymbol{\beta}}_i^a(h)$ and $\hat{\boldsymbol{\Sigma}}_{\boldsymbol{u}}$ as corresponding maximum likelihood estimators. From (17) we straightforwardly obtain the standard errors in (18) by correspondingly inserting the estimates $\hat{\boldsymbol{\beta}}_i^a(h)$ and $\hat{\boldsymbol{\Sigma}}_{\boldsymbol{u}}$.

The computation of the asymptotic variance of $\widehat{cir}_i(\boldsymbol{u}_\tau, h, \boldsymbol{d}) = \sum_{j=1}^h \hat{\boldsymbol{\beta}}_i(j)' \boldsymbol{d}$ is simplified by noting that

$$
\begin{aligned}
\operatorname{Cov}\left(\hat{\boldsymbol{\beta}}_i^a(h), \hat{\boldsymbol{\beta}}_i^a(h+j)\right) &= E\left(\left(\hat{\boldsymbol{\beta}}_i^a(h) - \boldsymbol{\beta}_i(\boldsymbol{A}, h)\right)\left(\hat{\boldsymbol{\beta}}_i^a(h+j) - \boldsymbol{\beta}_i(\boldsymbol{A}, h+j)\right)'\right) \\
&= E\left(\boldsymbol{u}_\tau \boldsymbol{u}_\tau'\right) E\left(\sum_{\tau}^{\tau-h} \xi_\tau \boldsymbol{u}_\tau \sum_{s}^{s-h} \xi_s \boldsymbol{u}_s'\right) \\
&= E\left(\boldsymbol{u}_\tau \boldsymbol{u}_\tau'\right) E\left(\sum_{\tau}^{\tau-h} \xi_\tau \boldsymbol{u}_\tau \sum_{s}^{s-h} \xi_s E\left(\boldsymbol{u}_s' \,|\{\boldsymbol{u}_l\}_{l>s}\right)\right) = 0.
\end{aligned}
$$

Consequently, we have $AV[\sum_{j=1}^h \hat{\boldsymbol{\beta}}_i^a(j)] = \sum_{j=1}^h AV[\hat{\boldsymbol{\beta}}_i^a(j)]$. Accordingly, the asymptotic variance of $\widehat{cir}_i(\boldsymbol{u}_\tau, h, \boldsymbol{d}) = \sum_{j=0}^h \hat{\boldsymbol{\beta}}_i(j)' \boldsymbol{d}$ follows from Equation (17), with $\hat{\boldsymbol{\beta}}_i^a(h)$ replaced by $\sum_{k=1}^h \hat{\boldsymbol{\beta}}_i^a(h)$, $ir_i(\boldsymbol{u}_\tau, h, \boldsymbol{d})$ replaced by $cir_i(\boldsymbol{u}_\tau, h, \boldsymbol{d})$ and $AV[\hat{\boldsymbol{\beta}}_i^a(h)]$ replaced by $\sum_{k=1}^h AV[\hat{\boldsymbol{\beta}}_i^a(h)]$. □

Proof. (Proposition 1) For ease of exposition, we derive the equilibrium quantities provided in Proposition 1 individually within the Lemmas below: Lemma 1 summaries price impact and net initiator volume for the baseline model, Lemma 2 derives the equivalent quantities for the risk aversion shock model and Lemma 3 concludes with the equilibrium quantities from the cash flow risk model. □

Proof. (Corollary 1) Follows directly from Proposition 1, Equations (24) - (26). Setting $z = 0$ and $s = \bar{D}$ we get $\nu = 0$, $\nu' = -\pi\left(1 - \frac{\bar{\alpha}}{\alpha'}\right)\bar{\theta} < 0$ and $\nu'' = \pi \frac{(1-b)\sigma''^2 \bar{\theta}}{\sigma^2}$. It holds that $(1-b) > 0$ because $0 < \beta_s < 1$ and $0 < \beta_\xi < 1$ by definition for σ''^2 such that $0 < b < 1$. □

Proof. (Corollary 2) Follows from Proposition 1, Equations (32) - (34). First, $\lambda > 0$ for $\pi < 1$

is trivial. Then, note that

$$\lambda' = \frac{\bar{\alpha}\sigma^2}{1-\pi+\pi\left(1-\frac{\bar{\alpha}}{\alpha'}\right)} = \frac{\bar{\alpha}\sigma^2}{1-\pi\frac{\bar{\alpha}}{\alpha'}} = \frac{\sigma^2}{\frac{1}{\bar{\alpha}}-\frac{\pi}{\alpha'}} = \frac{\alpha\sigma^2}{1-\pi} = \lambda \tag{1}$$

where in the second-to-last term we made use of $\bar{\alpha} := \frac{1}{(1-\pi)\frac{1}{\alpha}+\pi\frac{1}{\alpha'}}$. The final statement, $\lambda < \lambda''$, resembles the statement in Proposition 3.4 in Vayanos and Wang (2012). □

For ease of exposition, we start by presenting the equilibrium quantities of the baseline model as of see Section 2 of (Vayanos and Wang, 2012) (henceforth abbreviated to VW12). We always denote liquidity demanders with subscript d and liquidity suppliers with subscript s.

Lemma 1. *(Baseline model) Equilibrium quantities of the baseline model are*

$$\begin{aligned} v &= -\pi(1-\pi)z \\ \lambda &= \frac{\alpha\sigma^2}{1-\pi}. \end{aligned}$$

Proof. (Lemma 1) VW12 provide all proofs. Specifically, the following quantities are of relevance:

Agents' demand functions for the risky asset in Period 1 are $\theta_1^d = \frac{\bar{D}-S_1}{\alpha\sigma^2}$ and $\theta_1^d = \frac{\bar{D}-S_1}{\alpha\sigma^2} - z$ where market clearing implies that the period 1 equilibrium price is $S_1 = \bar{D} - \alpha\sigma^2\left(\bar{\theta}+\pi z\right)$.

Total initiator net volume as of VW12, Equation (2.15) is:

$$v = \pi\left(\frac{\bar{D}-S_1}{\alpha\sigma^2} - z - \bar{\theta}\right) = -\pi\left(1-\pi\right)z. \tag{2}$$

The price in Period 0 which includes the equilibrium discount for anticipated illiquidity is:

$$S_0 = S_0\left(\bar{\theta},\alpha,\sigma^2,\pi,\bar{D},\sigma_z^2\right) = \bar{D} - \alpha\sigma^2\bar{\theta} - \frac{\pi M}{1-\pi+\pi M}\Delta_1\bar{\theta}, \tag{3}$$

where

$$M = \exp\left(\tfrac{1}{2}\alpha\Delta_2\bar{\theta}^2\right)\sqrt{\frac{1+\Delta_0\pi^2}{1+\Delta_0(1-\pi)^2-\alpha^2\sigma^2\sigma_z^2}}, \tag{4}$$

$$\Delta_0 = \alpha^2\sigma^2\sigma_z^2, \tag{5}$$

$$\Delta_1 = \frac{\alpha\sigma^2\Delta_0\pi}{1+\Delta_0(1-\pi)^2-\alpha^2\sigma^2\sigma_z^2}, \tag{6}$$

$$\Delta_2 = \frac{\alpha\sigma^2\Delta_0}{1+\Delta_0(1-\pi)^2-\alpha^2\sigma^2\sigma_z^2}. \tag{7}$$

The price impact of the total initiator net volume is:

$$\lambda = \frac{\mathrm{Cov}(S_1-S_0,\nu)}{\mathrm{Var}(\nu)} = \frac{\mathrm{Cov}\left(\alpha\sigma^2\pi z, \pi(1-\pi)z\right)}{\sigma_z^2\pi^2(1-\pi)^2} = \frac{\alpha\sigma^2}{1-\pi} \tag{8}$$

□

Lemma 2. *(Risk aversion shock) Equilibrium quantities of the model with a risk aversion shock are*

$$\nu' = \nu - \pi\left(1-\frac{\bar{\alpha}}{\alpha'}\right)\left(\pi z+\bar{\theta}\right),$$
$$\lambda' = \frac{\bar{\alpha}\sigma^2}{1-\pi+\pi\left(1-\frac{\bar{\alpha}}{\alpha'}\right)}$$

Proof. (Lemma 2) A risk aversion shock is added to the baseline model by letting the fraction π of agents experiences a change of risk aversion from α to α'. The optimal holding of these agents after experiencing the shock becomes (VW12, Equation 2.4b):

$$\theta_1^{d\prime} = \frac{\bar{D}-S_1'}{\alpha'\sigma^2} - z, \tag{9}$$

where a prime is added to equilibrium quantities that change. The holdings for the liquidity providers remain like in the baseline model (WV12, Eq. 2.4a):

$$\theta_1^{s\prime} = \frac{\bar{D}-S_1'}{\alpha\sigma^2}. \tag{10}$$

Market clearing requires that demand equals supply such that

$$\pi\theta_1^{d\prime} + (1-\pi)\,\theta_1^{s\prime} = \bar{\theta}. \tag{11}$$

Plugging in delivers the Period 1 price:

$$S_1' = \bar{D} - \bar{\alpha}\sigma^2\left(\bar{\theta} + \pi z\right), \tag{12}$$

where

$$\bar{\alpha} = \frac{1}{(1-\pi)\,\frac{1}{\alpha} + \pi\frac{1}{\alpha'}}. \tag{13}$$

Note that the inverse of the economy's risk aversion coefficient in Period 1, $1/\bar{\alpha}$, is the weighted average of the inverted risk aversion coefficients of the two types of agents.

Total initiator net volume becomes

$$\begin{aligned}
\nu' &= \pi\left(\theta_1^{d\prime} - \bar{\theta}\right) = \pi\left(\frac{\bar{D} - S_1'}{\alpha'\sigma^2} - z - \bar{\theta}\right) \\
&= \pi\left(\frac{\bar{\alpha}}{\alpha'}\left(\bar{\theta} + \pi z\right) - z - \bar{\theta}\right) = \pi\left(\left(\frac{\bar{\alpha}}{\alpha'} - 1\right)\left(\bar{\theta} + \pi z\right)\right) - \pi z\,(1-\pi) \\
&= \nu - \pi\left(1 - \frac{\bar{\alpha}}{\alpha'}\right)\left(\pi z + \bar{\theta}\right).
\end{aligned} \tag{14}$$

Notice how for a sudden risk aversion shock, $\alpha' > \alpha$, initiator net volume becomes negative even in the absence of an endowment shock, and it becomes more sensitive to endowment shocks. If one sets the interim liquidity shock to its expectation, $z = 0$, initiator net volume in the baseline model becomes zero but turns negative for $\alpha' > \alpha$. In other words: After a risk aversion shock, liquidity demanders are net sellers of the risky asset, and they pay an additional liquidity premium of size $(\alpha' - \bar{\alpha})\,\sigma^2\bar{\theta} > 0$ to incentivize liquidity providers for holding more units of the risky asset.

Expected utility liquidity supplier. To extract the Period 0 price we follow the same steps as VW12 and update their equations as follows. First, note that $W_1 = W_0 + \theta_0\left(S_1' - S_0'\right) = W_0 + \theta_0\left(\bar{D} - S_0'\right) - \bar{\alpha}\sigma^2\theta_0\left(\bar{\theta} + \pi z\right)$. The expected utility of the liquidity supplier in Period 1 becomes (VW12, Equation 2.8):

$$= -E\left(\exp\left(-\alpha\left[W_1 + \theta_1^{s\prime}\left(D - S_1'\right)\right]\right)\right) \tag{15}$$

$$= -\exp\left(-\alpha\left[W_1 + \theta_1^{s\prime}\left(\bar{D} - S_1'\right) - \frac{1}{2}\alpha\sigma^2\left(\theta_1^{s\prime}\right)^2\right]\right) \tag{16}$$

$$= -\exp\left(-\alpha\left[W_0 + \theta_0\left(\bar{D} - S_0'\right) - \bar{\alpha}\sigma^2\theta_0\left(\bar{\theta} + \pi z\right) + \tfrac{1}{2}\tfrac{\bar{\alpha}^2}{\alpha}\sigma^2\left(\bar{\theta} + \pi z\right)^2\right]\right). \tag{17}$$

With the help of VW12 Lemma A.1, we compute the expected utility of a liquidity supplier *before* observing z (VW12, Equation A.2). The updated variables to be used when applying Lemma A.1 are (only changed variables are mentioned):

$$A' = W_0 + \theta_0\left(\bar{D} - S_0'\right) - \bar{\alpha}\sigma^2\theta_0\bar{\theta} + \tfrac{1}{2}\tfrac{\bar{\alpha}^2}{\alpha}\sigma^2\bar{\theta}^2, \tag{18}$$

$$B' = \sigma^2\pi\left(\tfrac{\bar{\alpha}^2}{\alpha}\bar{\theta} - \bar{\alpha}\theta_0\right), \tag{19}$$

$$C' = \tfrac{\bar{\alpha}^2}{\alpha}\sigma^2\pi^2. \tag{20}$$

The expected utility of a liquidity supplier becomes:

$$U^{s\prime} = -\exp\left(-\alpha F^s\right)\frac{1}{\sqrt{1 + \bar{\alpha}^2\sigma^2\sigma_z^2\pi^2}}, \tag{21}$$

where

$$F^{s\prime} = W_0 + \theta_0\left(\bar{D} - S_0'\right) - \bar{\alpha}\sigma^2\theta_0\bar{\theta} + \tfrac{1}{2}\tfrac{\bar{\alpha}^2}{\alpha}\sigma^2\bar{\theta}^2 - \alpha\frac{\sigma^4\sigma_z^2\pi^2\left(\tfrac{\bar{\alpha}^2}{\alpha}\bar{\theta} - \bar{\alpha}\theta_0\right)^2}{2\left(1 + \bar{\alpha}^2\sigma^2\sigma_z^2\pi^2\right)} \tag{22}$$

Expected utility liquidity demander. Following the same steps, we work towards computing the expected utility of a liquidity demander prior to observing z (VW12, Eq. A.4). Then, the expected utility of the liquidity demander in Period 1 is:

$$-\exp\left(-\alpha\left[W_1' + \theta_1^{d\prime}\left(\bar{D} - S_1'\right) - \tfrac{1}{2}\alpha'\sigma^2\left(\theta_1^{d\prime} + z\right)^2\right]\right), \tag{23}$$

where the adjusted alpha α' is used to compute the expected utility of Period 2 cash flow risk. Notice how any remaining uncertainty with respect to Period 1 price (due to z) is being evaluated with the unadjusted risk aversion α because this uncertainty will be experienced from Period 0 to Period 1 where agents have not yet learned their type (demander or supplier) and risk aversion therefore is alpha for both.

Inserting the equilibrium expressions for $\theta_1^{d\prime}$ from (9) and S_1' from (12), yields:

$$-\exp\left(-\alpha\left[W_0+\theta_0\left(\bar{D}-S_0'\right)-\bar{\alpha}\sigma^2\left(\theta_0+z\right)\left(\bar{\theta}+\pi z\right)+\tfrac{1}{2}\tfrac{\bar{\alpha}^2}{\alpha'}\sigma^2\left(\bar{\theta}+\pi z\right)^2\right]\right), \tag{24}$$

where z is the only addition to the expression for the liquidity supplier in Equation (17). The expected utility *before* observing z becomes is computed from Lemma A.1 (VW12) with the following updated variables:

$$A' = W_0+\theta_0\left(\bar{D}-S_0'\right)-\bar{\alpha}\sigma^2\theta_0\bar{\theta}+\tfrac{1}{2}\tfrac{\bar{\alpha}^2}{\alpha}\sigma^2\bar{\theta}^2, \tag{25}$$

$$B' = \sigma^2\pi\left(\tfrac{\bar{\alpha}^2}{\alpha'}\bar{\theta}-\bar{\alpha}\theta_0\right)-\bar{\alpha}\sigma^2\bar{\theta}, \tag{26}$$

$$C' = \bar{\alpha}\sigma^2\left(\tfrac{\bar{\alpha}}{\alpha'}\pi^2-2\pi\right), \tag{27}$$

where A', B', and C' are the same as the expressions for the liquidity supplier, except for the addition of the last term for B' and C' (which is the result of the additional z in Equation (24)).

The expected utility of a liquidity demander becomes:

$$U^{d\prime} = -\exp\left(-\alpha F^{d\prime}\right)\frac{1}{\sqrt{1+\alpha\bar{\alpha}\sigma^2\sigma_z^2\left(\frac{\bar{\alpha}}{\alpha'}\pi^2-2\pi\right)}}, \tag{28}$$

where

$$F^{d\prime} = W_0+\theta_0\left(\bar{D}-S_0'\right)-\bar{\alpha}\sigma^2\theta_0\bar{\theta}+\tfrac{1}{2}\tfrac{\bar{\alpha}^2}{\alpha}\sigma^2\bar{\theta}^2 - \alpha\frac{\sigma_z^2\left(\sigma^2\pi\left(\frac{\bar{\alpha}^2}{\alpha'}\bar{\theta}-\bar{\alpha}\theta_0\right)-\bar{\alpha}\sigma^2\bar{\theta}\right)^2}{2\left(1+\alpha\bar{\alpha}\sigma^2\sigma_z^2\left(\frac{\bar{\alpha}}{\alpha'}\pi^2-2\pi\right)\right)}. \tag{29}$$

Equilibrium price at time 0. The Period 0 agents chooses θ_0 to maximize:

$$U' = (1-\pi)\,U^{s\prime}+\pi U^{d\prime} \tag{30}$$

The associated first-order condition is:

$$(1-\pi)\exp\left(-\alpha F^{s\prime}\right)\left(-\alpha\frac{dF^{s\prime}}{d\theta_0}\right)\frac{1}{\sqrt{1+\bar{\alpha}^2\sigma^2\sigma_z^2\pi^2}} + \pi\exp\left(-\alpha F^{d}\right)\left(-\alpha\frac{dF^{d\prime}}{d\theta_0}\right)\frac{1}{\sqrt{1+\alpha\bar{\alpha}\sigma^2\sigma_z^2\left(\frac{\bar{\alpha}}{\alpha'}\pi^2-2\pi\right)}} = 0 \tag{31}$$

Let us compute the various parts of this equation and evaluate them in equilibrium (i.e., at $\theta_0 = \bar{\theta}$):

$$\frac{dF^{s\prime}}{d\theta_0} = \bar{D} - S_0' - \bar{\alpha}\sigma^2\bar{\theta} + \frac{\bar{\alpha}^2\sigma^4\sigma_z^2\pi^2(\bar{\alpha}-\alpha)}{1+\bar{\alpha}^2\sigma^2\sigma_z^2\pi^2}\bar{\theta} \tag{32}$$

$$F^{s\prime} = W_0 + \left(\bar{D} - S_0'\right)\bar{\theta} - \bar{\alpha}\sigma^2\bar{\theta}^2 + \tfrac{1}{2}\tfrac{\bar{\alpha}^2}{\alpha}\sigma^2\bar{\theta}^2 + \\ - \alpha\frac{\sigma^4\sigma_z^2\pi^2\bar{\alpha}^2\left(\frac{\bar{\alpha}}{\alpha}-1\right)^2}{2\left(1+\bar{\alpha}^2\sigma^2\sigma_z^2\pi^2\right)}\bar{\theta}^2 \tag{33}$$

$$\frac{dF^{d\prime}}{d\theta_0} = \bar{D} - S_0' - \bar{\alpha}\sigma^2\bar{\theta} + \alpha\frac{\bar{\alpha}\sigma^2\sigma_z^2\pi\left(\sigma^2\pi\left(\frac{\bar{\alpha}^2}{\alpha'}-\bar{\alpha}\right)-\bar{\alpha}\sigma^2\right)}{1+\alpha\bar{\alpha}\sigma^2\sigma_z^2\left(\frac{\bar{\alpha}}{\alpha'}\pi^2-2\pi\right)}\bar{\theta} \tag{34}$$

$$F^{d\prime} = W_0 + \left(\bar{D} - S_0'\right)\bar{\theta} - \bar{\alpha}\sigma^2\bar{\theta}^2 + \tfrac{1}{2}\tfrac{\bar{\alpha}^2}{\alpha}\sigma^2\bar{\theta}^2 \tag{35}$$

$$- \alpha\frac{\sigma_z^2\left(\sigma^2\pi\left(\frac{\bar{\alpha}^2}{\alpha'}-\bar{\alpha}\right)-\bar{\alpha}\sigma^2\right)^2}{2\left(1+\alpha\bar{\alpha}\sigma^2\sigma_z^2\left(\frac{\bar{\alpha}}{\alpha'}\pi^2-2\pi\right)\right)}\bar{\theta}^2 \tag{36}$$

Let us simplify notation in the spirit of VW12:

$$\frac{dF^{d\prime}}{d\theta_0} = \frac{dF^{s\prime}}{d\theta_0} - \Delta_1'\bar{\theta}, \tag{37}$$

$$F^{d\prime} = F^{s\prime} - \tfrac{1}{2}\Delta_2'\bar{\theta}^2, \tag{38}$$

where

$$\Delta_1' = \frac{\bar{\alpha}^2\sigma^4\sigma_z^2\pi^2(\bar{\alpha}-\alpha)}{1+\bar{\alpha}^2\sigma^2\sigma_z^2\pi^2} - \alpha\frac{\bar{\alpha}\sigma^2\sigma_z^2\pi\left(\bar{\alpha}\sigma^2-\sigma^2\pi\left(\frac{\bar{\alpha}^2}{\alpha'}-\bar{\alpha}\right)\right)}{1+\alpha\bar{\alpha}\sigma^2\sigma_z^2\left(\frac{\bar{\alpha}}{\alpha'}\pi^2-2\pi\right)}, \tag{39}$$

$$\Delta_2' = \alpha\frac{\sigma_z^2\left(\sigma^2\pi\left(\frac{\bar{\alpha}^2}{\alpha'}-\bar{\alpha}\right)-\bar{\alpha}\sigma^2\right)^2}{1+\alpha\bar{\alpha}\sigma^2\sigma_z^2\left(\frac{\bar{\alpha}}{\alpha'}\pi^2-2\pi\right)} - \alpha\frac{\sigma^4\sigma_z^2\pi^2\bar{\alpha}^2\left(\frac{\bar{\alpha}}{\alpha}-1\right)^2}{1+\bar{\alpha}^2\sigma^2\sigma_z^2\pi^2}, \tag{40}$$

so that, inserting (37) and (38) into (31) yields (notice how, among others, the factor $\exp(-\alpha F^{s\prime})$ drops out which avoids ending up with a non-linear equation in S_0):

$$\frac{dF^{s\prime}}{d\theta_0}\left(\frac{1-\pi}{\sqrt{1+\bar{\alpha}^2\sigma^2\sigma_z^2\pi^2}}+\frac{\pi\exp\left(\frac{1}{2}\alpha'\Delta_2'\bar{\theta}^2\right)}{\sqrt{1+\alpha\bar{\alpha}\sigma^2\sigma_z^2\left(\frac{\bar{\alpha}}{\alpha'}\pi^2-2\pi\right)}}\right)= \frac{\pi\exp\left(\frac{1}{2}\alpha\Delta_2'\bar{\theta}^2\right)}{\sqrt{1+\alpha\bar{\alpha}\sigma^2\sigma_z^2\left(\frac{\bar{\alpha}}{\alpha'}\pi^2-2\pi\right)}}\Delta_1'\bar{\theta}, \tag{41}$$

which can be simplified to

$$\frac{dF^{s\prime}}{d\theta_0}\left(1-\pi+\pi M'\right)=\pi M'\Delta_1'\bar{\theta}, \tag{42}$$

where

$$M' = \exp\left(\frac{1}{2}\alpha'\Delta_2'\bar{\theta}^2\right)\sqrt{\frac{1+\bar{\alpha}^2\sigma^2\sigma_z^2\pi^2}{1+\alpha\bar{\alpha}\sigma^2\sigma_z^2\left(\frac{\bar{\alpha}}{\alpha'}\pi^2-2\pi\right)}}. \tag{43}$$

Inserting (32) in (42) yields:

$$\begin{aligned}
\boxed{S_0'} &= \bar{D}-\bar{\alpha}\sigma^2\bar{\theta}+\frac{\bar{\alpha}^2\sigma^4\sigma_z^2\pi^2\left(\bar{\alpha}-\alpha\right)}{1+\bar{\alpha}^2\sigma^2\sigma_z^2\pi^2}\bar{\theta}-\frac{\pi M'}{1-\pi+\pi M'}\Delta_1'\bar{\theta} && (44)\\
&= \bar{D}+\left(\alpha\sigma^2\bar{\theta}-\alpha\sigma^2\bar{\theta}\right)-\bar{\alpha}\sigma^2\bar{\theta}+\frac{\bar{\alpha}^2\sigma^2\sigma_z^2\pi^2}{1+\bar{\alpha}^2\sigma^2\sigma_z^2\pi^2}\left(\bar{\alpha}-\alpha\right)\sigma^2\bar{\theta}-\frac{\pi M'}{1-\pi+\pi M'}\Delta_1'\bar{\theta} && (45)\\
&= \bar{D}-\alpha\sigma^2\bar{\theta}-\left(\bar{\alpha}-\alpha\right)\sigma^2\bar{\theta}+\frac{\bar{\alpha}^2\sigma^2\sigma_z^2\pi^2}{1+\bar{\alpha}^2\sigma^2\sigma_z^2\pi^2}\left(\bar{\alpha}-\alpha\right)\sigma^2\bar{\theta}-\frac{\pi M'}{1-\pi+\pi M'}\Delta_1'\bar{\theta} && (46)\\
&= \bar{D}-\alpha\sigma^2\bar{\theta}+\left(\frac{\bar{\alpha}^2\sigma^2\sigma_z^2\pi^2}{1+\bar{\alpha}^2\sigma^2\sigma_z^2\pi^2}-1\right)\left(\bar{\alpha}-\alpha\right)\sigma^2\bar{\theta}-\frac{\pi M'}{1-\pi+\pi M'}\Delta_1'\bar{\theta} && (47)\\
&= \bar{D}-\alpha\sigma^2\bar{\theta}-\frac{\left(\bar{\alpha}-\alpha\right)\sigma^2\bar{\theta}}{1+\bar{\alpha}^2\sigma^2\sigma_z^2\pi^2}-\frac{\pi M'}{1-\pi+\pi M'}\Delta_1'\bar{\theta} && (48)
\end{aligned}$$

Notice that this expression closely resembles VW12 Eq. (2.10) with the exception that the third term is an additional one.

Price impact. With the expression for initiator net volume and equilibrium prices, we can now compute the price impact λ' that liquidity demanders pay for their demand:

$$\lambda' = \frac{\mathrm{Cov}\left(S_1'-S_0',\nu'\right)}{\mathrm{Var}\left(\nu'\right)}. \tag{49}$$

Inserting (12), (14), and (44) into this expression we get:

$$\mathrm{Var}\left(\nu'\right) = \mathrm{Var}\left(-z\pi\left(1-\pi\frac{\bar{\alpha}}{\alpha'}\right)\right) = \sigma_z^2\pi^2\left(1-\pi\frac{\bar{\alpha}}{\alpha'}\right)^2 \tag{50}$$

$$\lambda' = \frac{\bar{\alpha}\sigma^2}{1-\pi\frac{\bar{\alpha}}{\alpha'}} = \frac{\sigma^2}{\frac{1}{\bar{\alpha}}-\frac{\pi}{\alpha'}} = \frac{\alpha\sigma^2}{1-\pi}. \tag{51}$$

□

Lemma 3. *(Cash flow shock) Equilibrium quantities of the model with a cash flow shock are*

$$\begin{aligned}\nu'' &= \pi\frac{(1-b)\,\sigma''^2\bar{\theta}}{\sigma^2} + \pi\frac{(\beta_s-b)}{\alpha\sigma^2}\left(s-\bar{D}\right) - \pi\left(1-\frac{bc}{\alpha\sigma^2}\right)z \\ \lambda'' &= \frac{\alpha\sigma^2\left(D|S_1\right)}{(1-\pi)\left(1-\frac{\beta_\xi}{b}\right)}\end{aligned}$$

where $\alpha' > \bar{\alpha} := \frac{1}{(1-\pi)\frac{1}{\alpha}+\pi\frac{1}{\alpha'}} > \alpha$ *and*

$$\begin{aligned}b &= \frac{\pi\sigma^2\left(D|S_1\right)\beta_s + (1-\pi)\,\sigma^2\beta_\xi}{\pi\sigma^2\left(D|S_1\right) + (1-\pi)\,\sigma^2} \\ c &= \alpha\sigma_\varepsilon^2 \\ \beta_s &= 1-\frac{\sigma^2}{\sigma''^2}, \\ \beta_\xi &= \frac{\sigma''^2}{\sigma''^2+\sigma_\varepsilon^2+c^2\sigma_z^2}, \\ \sigma^2\left(D|S_1\right) &= \beta_\xi\left(\sigma_\varepsilon^2+c^2\sigma_z^2\right).\end{aligned}$$

Proof. (Lemma 3)

We model the case of increased cash flow risk as one where dividend risk is increased for the (identical) agents in Period 0, and it is common knowledge that liquidity demanders learn the additional information in Period 1 when observing a private signal:

$$s = D + \varepsilon, \tag{52}$$

where ε is normal with mean zero and variance σ_ε^2, and is independent of D and z. Note that we do not land in a no-trade theorem, since these agents also trade due to an endowment shock (Milgrom and Stokey, 1982). The equilibrium quantities are presented in this subsection and denoted with a double prime. These quantities are developed in VW12 Sec. 3 where the baseline case corresponds to the no-information case discussed in VW12 Sec. 3.2). To consider the case of a Period 0 risk *increase* from the baseline model σ^2 to $\sigma^{2\prime\prime} > \sigma^2$, we set:

$$\sigma_\varepsilon^2 = \frac{\sigma^2 \sigma''^2}{\sigma''^2 - \sigma^2}, \tag{53}$$

so that the posterior risk for liquidity demanders after observing the signal s in Period 1 becomes (VW12 Equation 3.2b):

$$\sigma^2 (D|s) = \frac{\sigma_\varepsilon^2}{\sigma''^2 + \sigma_\varepsilon^2} \sigma''^2 = \sigma^2, \tag{54}$$

which is the baseline model cash flow risk. The liquidity demander who received the signal in Period 1 therefore experiences the same risk as the baseline model. The increased cash flow risk is experienced by the uninformed liquidity suppliers in Period 1, and, therefore, by all agents in Period 0 before they learn their type (i.e., liquidity demander or supplier).

With this reparametrization the equilibrium quantities are taken straight from VW12 Sec. 3 by, in their expressions, using:

$$\sigma^2 = \sigma''^2. \tag{55}$$

The equilibrium price in Period 1 is:

$$S_1 = a + b\left(s - \bar{D} - cz\right), \tag{56}$$

with

$$a = \bar{D} - \alpha (1 - b) \sigma^2 \bar{\theta}, \tag{57}$$

$$b = \frac{\pi \sigma^2 (D|S_1) \beta_s + (1 - \pi) \sigma^2 \beta_\xi}{\pi \sigma^2 (D|S_1) + (1 - \pi) \sigma^2}, \tag{58}$$

$$c = \alpha \sigma_\varepsilon^2 \tag{59}$$

$$\beta_s = \frac{\sigma''^2}{\sigma''^2 + \sigma_\varepsilon^2}, \tag{60}$$

$$\beta_\xi = \frac{\sigma''^2}{\sigma''^2 + \sigma_\varepsilon^2 + c^2 \sigma_z^2}, \tag{61}$$

$$\sigma^2 (D|S_1) = \beta_\xi \left(\sigma_\varepsilon^2 + c^2 \sigma_z^2\right). \tag{62}$$

The initiator net volume due to liquidity demanders is:

$$
\begin{aligned}
\nu'' &= \pi\left(\theta_1^d - \bar{\theta}\right) = -(1-\pi)\left(\theta_1^s - \bar{\theta}\right) \\
&= -(1-\pi)\left(\frac{\bar{D} + \beta_\xi / b\left(S_1'' - a\right) - S_1''}{a\sigma^2(D|S_1)} - \bar{\theta}\right)
\end{aligned} \tag{63}
$$

The Period 0 price is

$$
S_0'' = \bar{D} - \alpha\sigma''^2\bar{\theta} - \frac{\pi M''}{1-\pi+\pi M''}\Delta_1''\bar{\theta}, \tag{64}
$$

where M is given by (4) with the deltas replaced by:

$$
\Delta_0'' = \frac{\left(b-\beta_\xi\right)^2\left(\sigma''^2 + \sigma_\varepsilon^2 + c^2\sigma_z^2\right)}{\sigma^2\left(D|S_1\right)\pi^2}, \tag{65}
$$

$$
\Delta_1'' = \frac{\alpha^3 b\sigma''^2\left(\sigma''^2 + \sigma_\varepsilon^2\right)\sigma_z^2}{1 + \Delta_0''\left(1-\pi\right)^2 - \alpha^2\sigma''^2\sigma_z^2}, \tag{66}
$$

$$
\Delta_2'' = \frac{\alpha^3\sigma''^4\sigma_z^2\left(1 + \frac{(\beta_s - b)^2\left(\sigma''^2 + \sigma_\varepsilon^2\right)}{\sigma^2}\right)}{1 + \Delta_0''\left(1-\pi\right)^2 - \alpha^2\sigma''^2\sigma_z^2}. \tag{67}
$$

The price impact is:

$$
\lambda'' = \frac{\alpha\sigma^2\left(D|S_1\right)}{(1-\pi)\left(1 - \frac{\beta_\xi}{b}\right)}. \tag{68}
$$

□

II Details on the computation of Abel Noser institutional order flow

Abel Noser data does *not* provide information on the timing and volume of child orders as well as the types of orders executed by the broker. We discard *all* client transactions with recorded placement and execution times outside the regular (NASDAQ) trading hours.[9] Further, we only

[9]This requirement eliminates roughly 60% of all recorded client transactions. The remaining sample contains more than 220,000 executed client transactions. Institutional clients can choose to reveal timestamps associated with the execution of the meta order. If clients chose not to provide this information, Abel Noser defines placement to the opening auction and execution to the closing auction (e.g. Hu et al., 2018).

keep transactions which are executed within one trading day in our sample. Such a conservative constraint allows us to keep estimation error of actual intraday client net volume small.

Because Abel Noser client transactions only reveal the meta orders submitted to the clients brokers but not the actually executed transactions and corresponding timestamps, we have to rely on a proxy for $\textit{client net volume}_{t,\tau,i}$ on a trading day t during the last 5-minute interval up to the timestamp τ for ticker i. We compute the total trading volume of each client meta order l as $V_l = \textit{shares}_l \cdot \textit{price}_l$ where $\textit{shares}_l$ is the number of shares of the meta order and $\textit{price}_l$ is the average reported execution price per share. Then, we define the duration of a client meta order with identifier l from order placement time s_l until order execution e_l in minutes as $\Delta_l = e_l - s_l$. Table AII in the Appendix provides summary statistics for the client transactions. We assume that the execution is in proportion to the duration Δ_l until execution such that net trading volume of transaction l on execution date t within each minute is simply

$$\textit{net volume}_{l,\tau} = \frac{V_l \cdot \textit{side}_l}{\Delta_l} \text{ for } \tau \in [s_l, e_l] \text{ and 0 otherwise.} \tag{69}$$

Finally, aggregated $\textit{client net volume}_{t,\tau,i}$ is the net of buy and sell client volumes for each client transaction active in ticker i during the last 5-minute interval before timestamp τ such that if $N_{t,i}$ is the number of recorded client transactions for ticker i on day t, we define

$$\textit{client net volume}_{t,\tau,i} := \sum_{l=1}^{N_{t,i}} \textit{net volume}_{l,\tau}. \tag{70}$$

We merge the NASDAQ order book and the Abel Noser dataset to illustrate the responses of institutional client net volume to a *VIX* shock as well as a shock in *VRP* and *ERV*. To that end, we re-estimate the coefficients of the impulse response function based on the entire available sample (January 2009 until April 2013) where we impose a shock of one positive standard deviation in changes of either $IV_{t,\tau}$ or $ERV_{t,\tau}$ or $VRP_{t,\tau}$.